THE JOURNAL OF BIOLOGICAL CHEMISTRY VOL. 288, NO. 7, pp. 4522–4537, February 15, 2013

Fam57b (Family with Sequence Similarity 57, Member B), a Novel Peroxisome Proliferator-activated Receptor γ Target Gene That Regulates Adipogenesis through Ceramide Synthesis*

Received for publication, November 29, 2012, and in revised form, December 28, 2012 Published, JBC Papers in Press, December 28, 2012, DOI 10.1074/jbc.M112.440792

Yzumi Yamashita-Sugahara[1], **Yoshimi Tokuzawa, Yutaka Nakachi, Yukiko Kanesaki-Yatsuka, Masahito Matsumoto, Yosuke Mizuno, and Yasushi Okazaki**[2]

From the Division of Functional Genomics and Systems Medicine, Research Center for Genomic Medicine, Saitama Medical University, 1397-1 Yamane, Hidaka City, Saitama 350-1241, Japan

Background: *Fam57b* was identified as a putative novel PPARγ target up-regulated in adipocytes and adipose tissue.
Results: *Fam57b* was confirmed as a novel target of PPARγ by reporter and ChIP assays. FAM57B synthesizes ceramides and inhibits adipogenesis in mouse stromal ST2 cells.
Conclusion: FAM57B regulates adipogenesis through ceramide synthesis.
Significance: This study reveals one of the pleiotropic actions of PPARγ related to ceramide metabolism.

This report identifies a novel gene encoding *Fam57b* (family with sequence similarity 57, member B) as a novel peroxisome proliferator-activated receptor γ (PPARγ)-responsive transmembrane gene that is related to obesity. The gene was identified based on an integrated bioinformatics analysis of the following three expression profiling data sets: adipocyte differentiation of mouse stromal cells (ST2 cells), adipose tissues from obesity mice, and siRNA-mediated knockdown of *Pparγ* using ST2 cells. *Fam57b* consists of three variants expressed from different promoters and contains a Tram-Lag1-CLN8 domain that is related to ceramide synthase. Reporter and ChIP assays showed that *Fam57b* variant 2 is a *bona fide* PPARγ target gene in ST2 cells. *Fam57b* was up-regulated during adipocyte differentiation, suggesting that FAM57B is involved in this process. Surprisingly, FAM57B overexpression inhibited adipogenesis, and siRNA-mediated knockdown promoted adipocyte differentiation. Analysis of the ceramide content by lipid assay found that ceramides were in fact augmented in FAM57B-overexpressing ST2 cells. We also confirmed that ceramide inhibits adipogenesis. Therefore, the aforementioned results of FAM57B overexpression and siRNA experiments are reconciled by ceramide synthesis. In summary, we present *in vitro* evidence showing that PPARγ regulates *Fam57b* transcription during the adipogenesis of ST2 cells. In addition, our results suggest that PPARγ activation contributes to the regulation of ceramide metabolism during adipogenesis via FAM57B.

Metabolic syndrome, which is characterized by abdominal visceral obesity and dyslipidemia, increases the risk of type 2 diabetes and cardiovascular disease through chronic systemic inflammation and insulin resistance (reviewed in Refs. 1 and 2). Obese adipose tissue secretes increased levels of proinflammatory adipokines, including tumor necrosis factor α (TNFα) (3), monocyte chemoattractant protein-1 (MCP-1) (4, 5), and interleukin-6 (IL-6) (6, 7) as well as plasminogen activator inhibitor-1 (PAI-1) (8). On the other hand, obese adipose tissue has decreased secretion of anti-inflammatory factors, such as adiponectin, resulting in chronic inflammation.

PPARγ is a member of the nuclear receptor family and is a well known master regulator of adipocyte differentiation (9–11), which has been demonstrated both *in vitro* and *in vivo* (12). PPARγ is also a target of the insulin-sensitizing synthetic ligand thiazolidinedione class of drugs, including rosiglitazone and pioglitazone (13). These chemicals decrease the expression of insulin resistance-inducing adipokines, such as TNF-α, IL-1, and resistin, and increase the production of the insulin-sensitizing hormone, adiponectin (14, 15). Unfortunately, however, these PPARγ agonists also have adverse effects, such as body weight gain, liver dysfunction, and an increased risk of heart failure (16). Thus, it is important to identify new targets of PPARγ that offer a new pathway for the pleiotropic action of PPARγ. These specific targets may provide new therapeutic options to enhance the beneficial effects of PPARγ or decrease the side effects of PPARγ. Therefore, the objective of this study was to identify PPARγ target genes with particular emphasis on secretory or transmembrane genes that are related to metabolic syndrome or obesity.

To this end, we performed a gene expression analysis of adipose tissue in obese *versus* lean mice. We chose genes that were up-regulated more than 2-fold in obese mice relative to lean mice and that overlapped with genes up-regulated in ST2 cells during adipogenesis. We further narrowed down the genes by selecting those that were down-regulated in ST2 cells treated with *Pparγ*-targeting siRNA (si*Pparγ*). As a result, we identified 14 genes and ultimately focused on a novel gene, *Fam57b* (family with sequence similarity 57, member B) and analyzed its

* This work was supported in part by a grant-in-aid for the "Genome Network Project" (to Y. O.) and "Support Project of Strategic Research Center in Private Universities" from the Ministry of Education, Culture, Sports, Science, and Technology (MEXT) (to Saitama Medical University Research Center for Genomic Medicine).
[1] Recipient of the Saitama Medical University Research Fellowship.
[2] To whom correspondence should be addressed. Tel.: 81-42-984-0318; Fax: 81-42-984-0349; E-mail: okazaki@saitama-med.ac.jp.

TABLE 1
Primers used for subcloning

Primer	Sequence
pGcDNsam retrovirus cloning	
*Fam57b_var1*Fw	5′-gctctgagaagcggccgccatgcttaccccaatggtggctgggg
*Fam57b_var2*Fw	5′-gctctgagaagcggccgccatggccctgctcttcctgctg
Fam57b_var1(No tag)_Rv	5′-acgtcgactcagtcctgggtctgacaaggagagggtg
*Fam57b_var3*Fw	5′-gctctgagaagcggccgccatggcctccacagctggc
Fam57b_var1,2,3(FLAG)_Rv	5′-cgggatccgtcctgggtctgacaaggagagggtg
*pCMV5aFLAG*_Rv	5′-cgggatccctacttgtcatcgtcgtccttgtaatc
*pCMV5aNotag*_Rv	5′-ttccgcggccgctactcgagacgtcgacctacttgtcatcgtcgtccttgtaatc
*Cers2*_Fw	5′-gctctgagaagcggccgccatgctccagaccttgtatgactac
*Cers2*_Rv	5′-ttccgcggccgctatggccgacgtcgactcagtcattcttaggatgattgttattgagg
*Cers2FLAG*_Rv	5′-cgggatccgtcattcttaggatgattgttattgagg
pGL4.10 luc2 cloning	
*Fam57b*_pro1(PPRE) Fw1	5′-tggcctaactggccggtaccttctgaggaccagacgaggt
*Fam57b*_pro3(PPRE)Fw3	5′-ggggtaccctgggggtaattcagtggtg
*Fam57b*_pro5(PPRE)Rv	5′-gaagatctctgcgtggaggattagatgtg
*Fam57b*_pro4(PPERE)Rv2	5′-gaagatctctgctggggttaaaggtgagt
*Fam57b*_pro3(PPRE)Rv3	5′-gaagatctcccgattgtcactggaacctt
*Fam57b*_pro2(PPRE)Rv4	5′-gaagatctcccaggtccacagctacacag
*Fam57b*_pro2(PPRE)del Fw	5′-cagtactctgggctgggggtaattc
*Fam57b*_pro2(PPRE)del Rv	5′-agcccagagtactgactgtcccttc
*Fam57b*_pro2(PPRE) mut1Fw	5′-agtacttttataaagttaactgggctggg
*Fam57b*_pro2(PPRE) mut1Rv	5′-ctttataaaagtactgactgtcccttc
*Fam57b*_pro2(PPRE) mut2Fw	5′-gagaaattaaactgggctgggggtaattc
*Fam57b*_pro2(PPRE) mut2Rv	5′-ccagtttaatttctcccagtactgactg
Fam57b _pro2-5_Fw	5′-cggtacccagtggtgaaccaccacac
*Fam57b*_pro2_5_Rv	5′-caccactgggtaccggccagttaggc

function in detail. Interestingly, FAM57B has a Tram-Lag1-CLN8 (TLC)[3] domain that is related to acyl-CoA-dependent ceramide synthase (17), and this domain is present in ceramide synthases (CERS1 to CERS6) (18–23).

Ceramide functions as a second messenger in a variety of cellular events, including apoptosis and differentiation (24, 25). The ceramide levels in cells depend on the balance between the rate of ceramide synthesis and degradation. Ceramide is either produced by hydrolysis of sphingomyelin by neutral and acid sphingomyelinase (26) or synthesized *de novo* by serine palmitoyltransferase, followed by ceramide synthase. We hereby identified a novel PPARγ target gene, *Fam57b*, analyzed its function *in vitro*, and ultimately demonstrated that FAM57B interferes with adipogenesis by augmenting ceramide synthesis.

EXPERIMENTAL PROCEDURES

Materials—D-*erythro*-Sphinganine, fumonisin B1, and C20-ceramide were obtained from Cayman Chemical Co. C18-ceramide was from Toronto Research Chemicals (Ontario, Canada). C2- and C6-ceramide, palmitoyl-CoA(C16:0), stearoyl-CoA(C18:0), and diacylglycerol kinase were purchased from Sigma-Aldrich, whereas arachidoyl-CoA, behenoyl-CoA (C22:0), lignoceroyl-CoA (C24:0), and hexacosanoyl-CoA (C26:0) were obtained from Avanti Polar Lipids (Alabaster, AL), and defatted bovine serum albumin was purchased from British BioCell International, Ltd. (Cardiff, UK). SYBR Green PCR master mix and BioScript reverse transcriptase were obtained from Applied Biosystems (Bedford, MA) and Bioline (London, UK), respectively. pGL4.10, pGL4.74, and the Dual-Luciferase reporter assay system were from Promega Corp. (Madison, WI). Restriction enzymes and DNA-modifying enzymes were from either Takara Bio (Otsu, Japan) or New England Biolabs (Beverly, MA). The anti-FLAG monoclonal antibody (clone M2) and 3× FLAG peptide were from Sigma-Aldrich. Silica gel 60 thin layer chromatography plate was from Whatman (Kent, UK). All solvents were of analytical grade and were purchased from Nacalai Tesque (Kyoto, Japan). Oligonucleotides were synthesized by Sigma-Aldrich and Invitrogen. [γ-^{32}P]ATP was obtained from PerkinElmer Life Sciences.

Expression Microarray Analysis—Total RNA was extracted from the adipose tissue of mice fed a normal diet (CE-2) or high fat diet (HFD32) (Clea, Tokyo, Japan) using a Nucleospin RNA II isolation kit (Macherey-Nagel, Düren, Germany) according to the manufacturer's instructions. Biotin-labeled cRNA was synthesized as recommended by the Affymetrix guidelines. The labeled samples were hybridized to Affymetrix GeneChip Mouse Genome 430 2.0 arrays according to the manufacturer's protocol. Scanning and intensity data analysis were performed as described previously (27). The raw data are publicly available at Gene Expression Omnibus (see the National Institutes of Health Web site) by accession number GSE36492. The data sets of ST2 cell adipocyte and si*Pparγ*-treated ST2 cell adipocyte are publicly available at the Genome network platform (see the National Institute of Genetics (Japan) Web site).

Molecular Cloning—Mouse cDNA was used as a template to amplify *Fam57b* variants 1, 2, and 3 as well as the *Cers2* open reading frame. A FLAG epitope was introduced at the 3′ terminus of mouse *Fam57b* by PCR. The PCR product was cloned into the pGcDNAsamIRES-EGFP retroviral vector (kindly provided by Masafumi Onodera (NCCHD, National Institutes of Health), and EGFP was deleted from FAM57B-pGcDNsamIRES-EGFP retroviral vectors using the ClaI and XhoI restriction enzymes. The primers used to generate the retroviral vector are described in Table 1.

[3] The abbreviations used are: TLC, Tram-Lag1-CLN8; CERS, ceramide synthase; PPRE, PPARγ-responsive element; qPCR, quantitative real-time PCR; qRT-PCR, quantitative real-time RT-PCR; FB1, fumonisin B1; EGFP, enhanced green fluorescent protein.

TABLE 2
Primers used for quantitative real-time PCR

	Forward	Reverse
ChIP-qPCR		
*Fam57b_var2*_1	5′-tggcctaactggccggtaccttctgaggaccagacgaggt	5′-aagatggagacgggaggact
*Fam57b_var2*_2	5′-aaacgtatttctgtggctcc	5′-taagatccgattgtcactgg
*Fam57b_var1*_1	5′-aagagaagagccatcctttcc	5′-gggaggcccttaaagagaca
*Fam57b_var1*_2	5′-tgcatcttcctcctcctgtc	5′-gacagagcgctggtgagag
*Fam57b_var3*_1	5′-cgagagttcagcccctctct	5′-atgaggtccaaggagggaag
*Fam57b_var3*_2F	5′-caaggggcaagactgtgttt	5′-cttaccatggccctcttcct
mRNA qRT-PCR		
*Fam57b_c*2	5′-ggctacctgcacaaggagtt	5′-aatctcccttgccttgtcg
Fam57b_var1(a)	5′-cccggactcttcctcctatc	5′-gcttggacagaggacaccaa
Fam57b_var2(a)	5′-ctgcagaatcgaaccagctt	5′-atgatggcttggacagagga
Fam57b_var3(a)	5′-agacgcacacctgattgtca	5′-cagccagtgctggtcatcta
Fam57b_var2(b)	5′-ctgctggggtgtgtcttctt	5′-cttgcctctccatccgtaag
Fam57b_var1(b)	5′-tgcatcttcctcctcctgtc	5′-gacagagcgctggtgagag
Cers2	5′-cgagatgctccagaccttgt	5′-tgtcttctagatcagcccaggt
Cers4	5′-tgcgatgctctcttcatcat	5′-cccgagttcttgatggagtc
Cers5	5′-catgccatctggtcctacct	5′-catcactgcggtcatcctta
Cers6	5′-gggttgaactgcttctggtc	5′-tcaatgtcactccggtcatc
PPARγ2	5′-atgggtgaaactctgggaga	5′-gagctgattccgaagttggt
Adipoq	5′-gatggcactcctggagagaa	5′-gcttctccaggctctccttt
Glut4	5′-gacggacactccatctgttg	5′-gccacgatggagacatagc
Plin1	5′-tgctggatggagacctc	5′-accggctccatgctcca
Gapdh	5′-tggagaaacctgccaagtatg	5′-ggagacaacctggtcctcag

Cell Culture and Infection—Mouse bone marrow-derived stromal cell line ST2 cells were obtained from the RIKEN BioResource Center (Tsukuba, Japan) and cultured as described previously (28). ST2 cells were grown in RPMI 1640 medium. 293FT cells, Plat-E cells (kindly provided by Toshio Kitamura (Institute of Medical Science)) and NIH3T3 cells were grown in Dulbecco's modified Eagle's medium (with high glucose, L-glutamine, sodium pyruvate, and pyridoxine hydrochloride). All media were supplemented with 10% fetal bovine serum (FBS), 100 IU/ml penicillin, and 100 IU/ml streptomycin. 293FT cells were cultured in medium supplemented with 500 μg/ml G418, and the culture medium for Plat-E cells was supplemented with 10 μg/ml blasticidin, 1 μg/ml puromycin, and MEM non-essential amino acids. The media and FBS were purchased from Nacalai Tesque and JRH BIO (St. Louis, MO), respectively. Cells were cultured at 37 °C with 5% CO_2. Viruses were prepared as described previously (29). Briefly, Plat-E cells were transfected with a mixture of viral plasmids, and the medium was replaced 24 h post-transfection. The viral supernatants were collected at 48, 72, and 96 h and then filtered. ST2 cells were incubated with the viral supernatants for 24 h, after which the cells were cultured in normal medium and then induced to undergo adipocyte differentiation 3 days after infection.

Adipogenic Differentiation—The adipogenic differentiation of ST2 cells was induced by changing the medium to differentiation medium supplemented with 0.5 mM 3-isobutyl-1-methylxanthine, 0.25 μM dexamethasone, and insulin-transferrin-selenium-X supplement containing 5 μg/ml insulin (Invitrogen). For ST2 cells that were treated with siRNA or transduced with retrovirus to overexpress FAM57B, 1 μM and 0.1 μM rosiglitazone, respectively, was also added to the medium. After 48–72 h, the differentiation medium was replaced with normal culture medium.

Effects of Ceramide on Differentiating ST2 Cells—ST2 cells were differentiated into adipocytes using an adipogenic hormonal mixture containing 5, 10, or 25 μM C6-ceramide, 20 or 25 μM C18-ceramide, and 7 or 15 μM C20-ceramide. C6-ceramide was solubilized in 100% ethanol, whereas C18- and C20-ceramides were solubilized in a 2% dodecane-EtOH solution as described previously (30). Ethanol and dodecane-EtOH were added to the control samples to adjust the concentration to each corresponding sample. On day 6, Oil Red O staining was performed to evaluate lipid accumulation in differentiating ST2 cells.

ChIP-Quantitative Real-time PCR (qPCR) Analysis—ChIP was performed as previously described (31). ST2 cells were allowed to differentiate into adipocytes and then fixed at 2 and 6 days post-differentiation. Undifferentiated samples were also prepared and analyzed at 6 days. An anti-PPARγ antibody (Santa Cruz Biotechnology, Inc. (Santa Cruz, CA) and PPMX (Tokyo, Japan)) was used for the ChIP assays. The ChIP samples were analyzed by real-time PCR using the primer indicated in Table 2. The results were normalized to cyclophilin levels in control DNA and presented as -fold enrichment of the PPARγ binding region.

Luciferase Reporter Assay—The *Fam57b* variant 2 promoter regions were cloned by PCR from the mouse genome (Table 1), and the cloned fragments were ligated into the promoterless plasmid pGL4.10 harboring the firefly luciferase gene. NIH3T3 cells were co-transfected with the firefly luciferase reporter vectors, expression vectors, and the internal control *Renilla* luciferase vector pGL4.74 using Lipofectamine 2000 (Invitrogen). At 24 h post-transfection, the cells were induced with 1 μM rosiglitazone for 24 h. The luciferase activity was measured using a Wallac 1420 multilabel counter (ARVO) (PerkinElmer Life Sciences). These experiments were performed more than three times.

Electrophoretic Mobility Shift Assay (EMSA)—EMSA was performed as described previously (32). DNA probes were prepared by end-labeling double-stranded oligonucleotides with T4 polynucleotide kinase and [γ-^{32}P]ATP (6000 Ci/ml). For the second PPRE of *Fam57b* variant 2 (var2), wild type (WT) and mutant type 1 (mut1) sequences were prepared. The oligonucleotides used in this study are listed in Table 3. Two micrograms of nuclear extract from preadipocyte or adipocyte-differ-

TABLE 3
Oligonucleotides used for EMSA

	Forward	Reverse
*aP2*PPRE	5′-cttcttactggatcagagttcactagtgg	5′-ttccactagtgaactctgatccagtaaga
*Fam57b*2up_PPRE2wt	5′-cacagtactgggagaaagttaactgggctg	5′-cccagcccagttaactttctcccagtactg
*Fam57b*2up_PPRE2mt1	5′-cacagtacttttataaagttaactgggctg	5′-cccagcccagttaactttataaaagtactg

TABLE 4
siRNA sequences

	Forward	Reverse
si*Fam57b*-A	5′-uauaggccgaggacagccagugcug	5′-cagcauggcuguccucggccuaua
si*Fam57b*-B	5′-ucaacaugcagccuagaaagaaauc	5′-gauuucuuuucuaggcugcauguuga
si*Fam57b*-C	5′-uuaaccuggugcuugugccaguggc	5′-gccacuggcacaagcaccagguuaa
si*Pparγ*	5′-aucuaauuccagugcauugaacuucac	5′-gaaguucaaugcacuggaauuagat

entiated ST2 cells were used for the binding reaction. After the binding reaction, the supershift assay was performed by adding 0.2 μg of a mouse monoclonal anti-PPARγ antibody (E8) (Santa Cruz) or 0.2 μg of a mouse control IgG (Santa Cruz Biotechnology, Inc.) for 20 min before loading the DNA-protein complex on a 6% native acrylamide gel in 0.5× TBE buffer.

Isolation of Total RNA and Quantitative Real-time RT-PCR (qRT-PCR)—Total RNA was isolated and qualified as described previously (33). Gene expression level was measured by qRT-PCR as previously described (28). The sequences of the forward and reverse primers used to amplify each gene are described in Table 2.

siRNA-mediated Knockdown of Fam57b—siRNAs targeting the mouse *Fam57b* transcript were purchased from Invitrogen. Negative Universal Control Med#2 (Invitrogen, catalog no. 12935-112) was used as a negative control, and si*Pparγ* was from IDT (Coralville, IA). The siRNA sequences for *Fam57b* are described in Table 4. For siRNA transfection, a complex of Lipofectamine 2000 and 20 nM siRNA was prepared according to the manufacturer's instructions and directly mixed with 6.4×10^4 cells in 24-well culture plates. The medium was replaced at 4–6 h post-transfection with fresh differentiation medium (adipogenic induction medium).

Lipid Assay—Lipid accumulation in adipocytes was detected based on Oil Red O staining, and the triglyceride content in adipocytes was determined as described previously (33, 34). ST2 cells differentiated into adipocytes with overexpressed FAM57B or with *Fam57b* siRNA at day 6 were fixed or extracted for further lipid assays. The ceramide content of ST2 adipocytes was determined as described previously (35). Lipids were extracted using the Bligh Dyer method, and then the ceramide content was measured using the diacylglycerol kinase method. The ceramide content was normalized to the protein levels. The extracted lipids were labeled with ^{32}P, converting the ceramide to ceramide 1-phosphate, and then separated by a thin layer chromatography plate using the following solvents: chloroform/acetone/methanol/acetic acid/water (30:12:9:6:3). The signals were counted with a BAS5000 imaging analyzer (FUJIFILM, Tokyo, Japan). A sphingomyelinase assay was performed using a sphingomyelinase assay kit (Cayman Chemical) according to the manufacturer's instructions. Briefly, total sphingomyelinase activity was analyzed using ST2 cells overexpressing FAM57B, the same conditions as for the ceramide content analysis. All experiments were performed at least three times.

Ceramide Synthase Activity Assay—This assay was performed as described previously (20). Differentiated ST2 cells overexpressing FAM57B-FLAG or 293FT cells that had been transiently transfected with FAM57B-FLAG were washed with PBS and harvested from culture dishes using a cell scraper. After centrifuging for 4 min at 150 × *g*, the cell pellets were homogenized in 20 mM HEPESKOH, pH 7.4, 25 mM KCl, 250 mM sucrose, and 2 mM $MgCl_2$ containing a protease inhibitor mixture (Nacalai Tesque), and the protein levels were measured. An anti-FLAG antibody was used to pull down FAM57B-FLAG from lysates of ST2 cells or 293FT cells overexpressing FAM57B-FLAG. The bound FAM57B-FLAG protein was released with 3× FLAG peptide according to the manufacturer's instructions. Homogenates (500 μg of protein/ml) or purified protein (5 μg of protein) were incubated with 15 μM sphingosine, 20 μM defatted-bovine serum albumin with or without 20 μM fumonisin B1 (FB1) for 5 min at 37 °C. The reaction was initiated by adding either 50 μM palmitoyl-CoA (C16), stearoyl-CoA (C18), or arachidoyl-CoA (C20) and then incubated for 1 h at 37 °C. Lipids were extracted, subjected to the diacylglycerol kinase assay, and analyzed as described above, except for the following change in the developing solvent system: CHCl3/acetone/MeOH/HOAc/H_2O (50:30:10:6:3). These experiments were performed more than three times.

Animals—All mice used in this study were maintained and handled according to protocols that were approved by the Animal Research Committee of Saitama Medical University.

RESULTS

Fam57b Was Identified as a Novel PPARγ Target Gene Using a Computational Analysis—To explore novel PPARγ target genes encoding secretory or transmembrane proteins that could represent new therapeutic targets, we performed an integrative analysis of three gene expression profile data sets: 1) ST2 cell-derived adipocytes during the course of differentiation at 0, 1, 2, 3, 4, 5, 6, 8, 10, 12, and 14 days; 2) adipose tissue obtained from mice fed a high fat diet and a normal diet as a control; and 3) ST2 cells treated with si*Pparγ* during adipogenesis and examined on day 5. A total of 642 genes were up-regulated in adipose tissue derived from mice fed a high fat diet compared with the control, 2300 were up-regulated in ST2 cell-derived adipocytes, and 517 genes were down-regulated in si*Pparγ*-treated ST2 cells. Of these, 24 genes overlapped across the three data sets, and ultimately 14 genes were extracted as secretory or transmembrane genes using the signal peptide (*SP*) or trans-

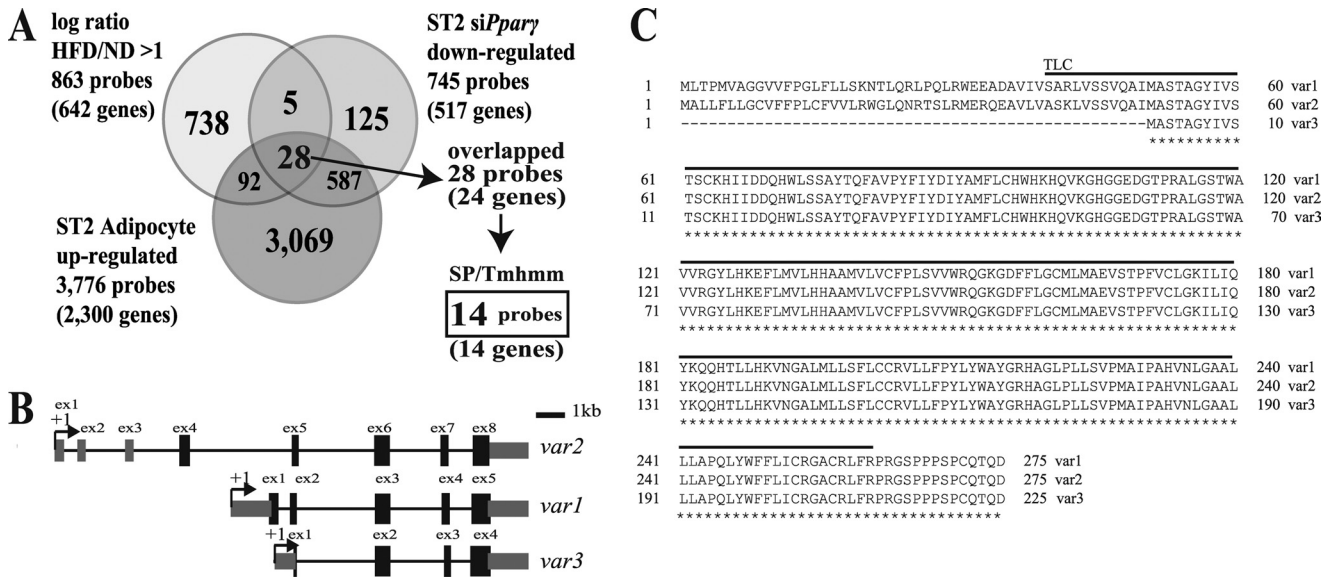

FIGURE 1. **Screening of PPARγ target genes that regulate metabolic disease.** *A*, we performed an expression analysis of genes under the following three conditions: 1) genes that were up-regulated more than 2-fold in adipose tissue from mice that were fed a high fat diet (*HFD*) compared with a normal diet as a control (*ND*), 2) genes up-regulated in ST2 cells that had undergone adipogenesis, and 3) genes down-regulated in ST2 cells that had been treated with siRNA targeting *Pparγ* and undergone adipogenesis. The *number* in the Venn diagram represents the number of probes on the microarray. There were 14 common genes that contained a signal sequence and/or transmembrane region (which was screened with the signal peptide (*SP*) and transmembrane hidden Marcov method (*Tmhmm*) programs) as shown in Table 5. *B*, the structures of three variants of the *Fam57b* gene. The last four exons are common exons in these three variants. *+1*, transcription start site. *C*, the common amino acid sequence of the three FAM57B variants is indicated with a *star below* each amino acid, in which the *lined* amino acid sequence indicates the TLC domain. The sequences were obtained from the NCBI Web site.

TABLE 5

The 14 genes extracted by the expression array based on an integrated analysis

Gene symbol	Accession number	Description
Dio2	NM_010050	Type II iodothyronine deiodinase
Clstn3	NM_153508	Calsyntenin-3 precursor
Ltc4s	NM_008521	Leukotriene C4 synthase
Ly6h	NM_011837	Lymphocyte antigen 6H isoform a precursor
Abcg1	NM_009593	ATP-binding cassette sub-family G member 1
Scd2	NM_009128	Acyl-CoA desaturase 2
Pnpla2	NM_001163689	Patatin-like phospholipase domain-containing protein 2 isoform 1
Mosc1	NM_001081361	MOSC domain-containing protein 1, mitochondrial
Lamb3	NM_008484	Laminin subunit β-3 precursor
Trfr2	NM_015799	Transferrin receptor protein 2
Cd53	NM_007651	Leukocyte surface antigen CD53
1100001G20Rik	NM_183249	WDNM1-like protein precursor
Dhcr7	NM_007856	7-Dehydrocholesterol reductase
Fam57b	NM_026884	Family with sequence similarity 57, member B

membrane hidden Marcov method (*Tmhmm*) program (Fig. 1*A* and Table 5). Four of these genes were previously identified as PPARγ targets (*Dio2*, *Abcg1*, *Pnpla2*, and *1100001G20Rik*) (36–38), five have been linked to lipid metabolism (*Scd2*, *Abcg1*, *Pnpla2*, *Mosc1*, and *Dhcr7*) (39–41), two have been related to inflammatory cells (*Ltc4s* and *Cd53*) (42, 43), and three have been identified as transmembrane proteins (*Ly6h*, *Trfr2*, *Cd53*, and *Clstn3*) (44–46). Because *Fam57b* has neither been functionally characterized nor previously reported but contains an interesting domain, the TLC domain, that is related to lipid metabolism (Fig. 1*C*) (47), we focused on this gene and performed a detailed characterization. LAG1 was first identified in yeast as essential for fatty acyl-CoA-dependent ceramide synthesis (17). *Fam57b* consists of three variants (variant 1 (var1), NM_029978.1; variant 2 (var2), NM_026884.1; variant 3 (var3), NM_001146347.1) that use different promoters (Fig. 1*B*) and have different N-terminal sequences but share a common TLC domain (Fig. 1*C*). Variant 3 has five whereas variants 1 and 2 have six putative transmembrane regions that were predicted using SOSUI (48). Variants 2 and 3 were experimentally shown to localize at the ER, whereas variant 1 localized at the Golgi (data not shown), which is consistent with the prediction that FAM57B is a transmembrane protein.

Expression Analysis of the Three Fam57b Variants—We analyzed the gene expression profile of the *Fam57b* variants in ST2 cells during adipogenesis as well as in different tissues and adipose tissue derived from obese or lean mice using qRT-PCR. All three *Fam57b* variants were up-regulated in ST2 and 3T3L1 cells during adipogenesis (Fig. 2, *A* and *B*). An analysis of different tissues showed a distinct expression profile for each variant across different tissues (*i.e.* variant 1 was highly up-regulated in the brain, whereas variant 2 was highly expressed in the testis and adipose tissue) (Fig. 2*D*). Interestingly, only variant 2 was expressed at higher levels in the adipose tissue of epididymal fat from obese mice compared with lean mice. The expression levels of variants 1 and 3 were significantly less in obese mice compared with lean mice (Fig. 2*E*). Thus, it is likely that FAM57B variant 2 has an important role in adipose tissue of obese mice.

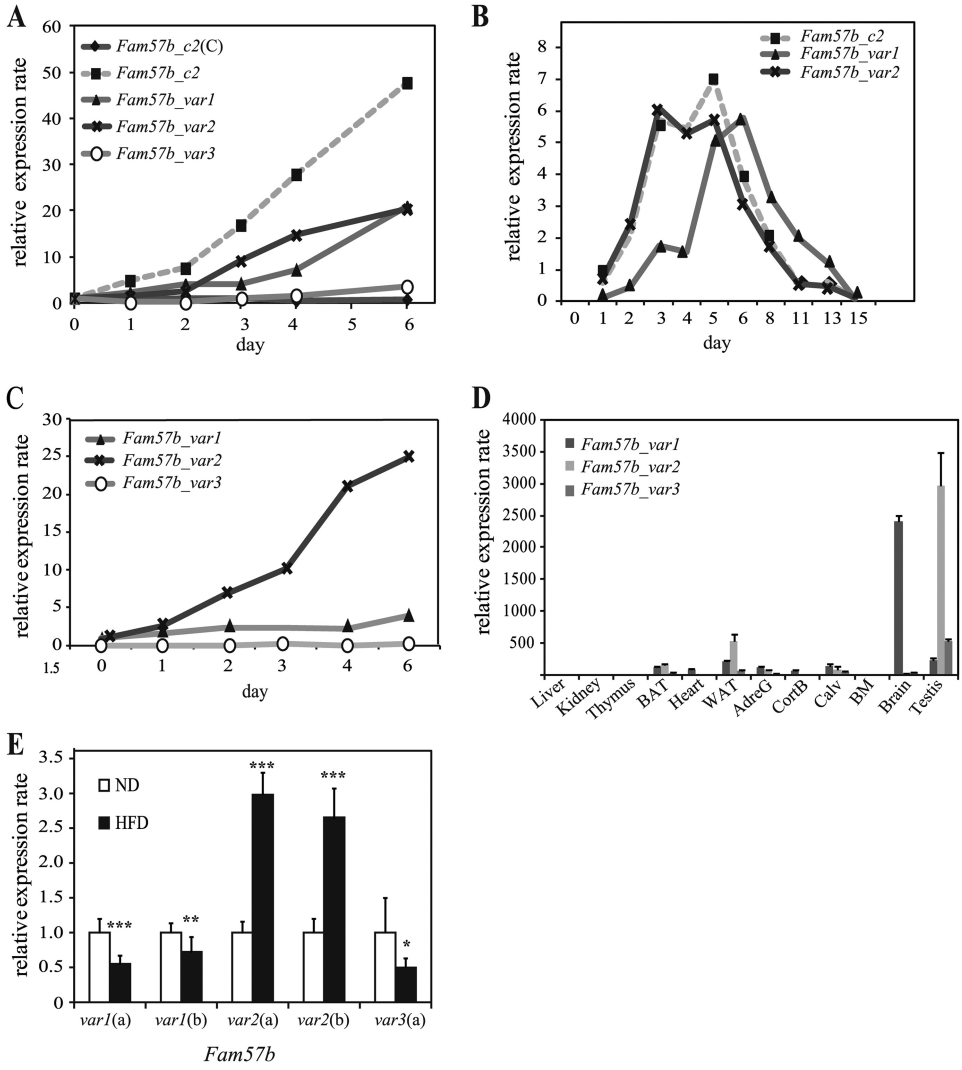

FIGURE 2. **Expression profiling of *Fam57b* in ST2 adipogenesis and mouse different tissues.** *A*, samples were harvested on the indicated days after adipogenic induction, and total RNA was extracted and analyzed by real-time RT-PCR with primers targeting a common sequence (indicated by *Fam57b_c2*) and variant-specific sequences (indicated by *Fam57b_var1*, *-2*, and *-3*). As a control, samples left uninduced were also analyzed by qRT-PCR using the common sequence primers (*Fam57b_c2*(C)). *B*, 3T3L1 cells were differentiated into adipocytes, and samples were harvested on the indicated days. Total RNA was extracted and analyzed for *Fam57b* expression using common primers (*Fam57b_c2*) as well as specific primers for variants 1 and 2 (*Fam57b_var1* and *Fam57b_var2*). *C*, ST2 cells were induced with rosiglitazone instead of a total adipogenic mixture and analyzed on the indicated days of differentiation. The mRNA expression of three *Fam57b* variants was analyzed by real-time RT-PCR as indicated above. *D*, the expression of the *Fam57b* variants in normal tissues from C57bBL/6J mice was analyzed by real-time RT-PCR with variant-specific primers. *BAT*, brown adipose tissue; *WAT*, white adipose tissue; *AdreG*, adrenal gland; *CortB*, cortical bone; *Calv*, calvaria; *BM*, bone marrow. *E*, the expression of the *Fam57b* variants was examined in adipose tissue derived from obese mice induced by a high fat diet (*HFD*), and from mice fed a normal diet (*ND*). Two different primers were used for variants 1 and 2 (*a* and *b*). Results are the means ± S.D. (*error bars*) ($n = 3$). *, $p < 0.05$; **, $p < 0.01$; ***, $p < 0.001$.

Fam57b Variant 2 Is a Bona Fide Novel Target of PPARγ—Because *Fam57b* was identified as a down-regulated gene in si*Pparγ*-treated cells, which suggests that *Fam57b* is a direct target of PPARγ, we validated whether *Fam57b* is directly regulated by PPARγ. An *in silico* analysis showed that PPARγ-responsive elements (PPREs) are located near the promoter regions of all *Fam57b* variants (indicated with *arrows* in Fig. 3*A*). To further determine whether these PPREs are regulated by PPARγ, we performed ChIP-qPCR for the three variants using two primer sets for each variant (as shown in Fig. 3*A*, in which the PCR primer site is indicated with a *heavy black line*; see also Table 2 for primer information). Unexpectedly, the ChIP-qPCR analysis of ST2 cells during adipocyte differentiation demonstrated that only the promoter region of variant 2 was enriched by PPARγ as much as ~20-fold compared with the input, as was *Fabp4* (fatty acid-binding protein (*ap2*)) by ~50-fold (Fig. 3*B*). These results indicate that variant 2 was occupied by PPARγ in adipocytes on days 2 and 6 post-differentiation but not in preadipocytes. Next, we performed a reporter assay with the promoter of *Fam57b* variant 2, which contained five candidate PPRE sequences. We cloned the promoter region of *Fam57b* variant 2 containing five PPREs into the pGL4.10 vector, and subclones with various deletions in this promoter were prepared (Fig. 4*A*). The luciferase reporter assay demonstrated that the construct containing five PPREs (pro1–5) showed up-regulation of luciferase activity by rosiglitazone. The luciferase activity was up-regulated as long as the second PPRE was present in the constructs (pro1–4, pro1–3,

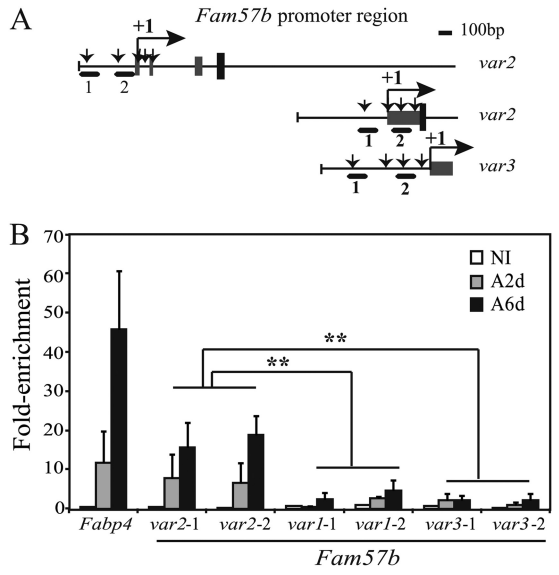

FIGURE 3. **PPARγ targets a promoter-proximal site of the *Fam57b* variant 2.** *A*, the predicted PPRE sequence sites are indicated with *arrows* on each *Fam57b* promoter, and *heavy lines* indicate the PCR amplicons used for ChIP-qPCR, whose numbers correspond to those indicated in Table 2. *B*, ST2 cells that were induced into adipocytes for 2 and 6 days (*A2d* and *A6d*, respectively) as well as uninduced cells were analyzed by ChIP-qPCR as indicated. *Fabp4* was used as a positive control, and the promoter site of each *Fam57b* variant was examined. Results are means ± S.D. (*error bars*) ($n = 3$); **, $p < 0.01$. *+1*, transcription start site.

pro1–2, and pro2–5). Thus, only the construct with pro3–5, lacking the second PPRE, resulted in luciferase not being activated by rosiglitazone (Fig. 4*B*), suggesting that the second PPRE is the critical site targeted by PPARγ in response to rosiglitazone. To confirm this finding, we constructed two mutants of the second PPRE (mut1 and mut2) and one deletion of the second PPRE in the construct pro1–5 (Fig. 4*A*). An analysis using these constructs demonstrated that luciferase activity was not up-regulated by rosiglitazone (Fig. 4*C*), indicating that a novel PPRE sequence in *Fam57b* variant 2, GGGAGAAAGTTAA (second PPRE at −132 to −120 bp) (WT) was targeted directly by PPARγ. To further determine whether PPARγ binds directly to this sequence, we performed EMSA. As shown in Fig. 4*D*, a specific DNA-binding activity was detectable with the WT PPRE sequence from the *Fam57b* variant 2 and *ap2* PPRE as probes when adipocyte nuclear extracts (*Ad NE*) were used (*lanes 5* and *7*). DNA-binding activity was not detected using preadipocyte nuclear extracts (*Pread NE*) (*lanes 2* and *4*). When either preadipocyte or adipocyte nuclear extracts were used, a distinct mobility shift in radioactivity with a mutant PPRE probe (mut1) was detectable (*lanes 3* and *6*, respectively), which is indicative of nonspecific DNA-binding activity. The DNA-binding activity with WT PPRE in *lane 5* was supershifted with an anti-PPARγ antibody (*lane 9*), indicating that PPARγ binds directly to this second PPRE.

Overexpressing or Knocking Down FAM57B in ST2 Cells Affects Adipocyte Differentiation—Because *Fam57b* is up-regulated during adipogenesis, we hypothesized that FAM57B promotes adipogenesis. To verify the *in vitro* effects of FAM57B on adipogenesis, we cloned three *Fam57b* variants with and without a C-terminal FLAG tag in a retroviral vector (with IRES-EGFP) and then overexpressed these variants in ST2 cells and assessed the effect on day 6 after adipocyte differentiation. The expression of each FAM57B-FLAG variant (var1F, -2F, and -3F) in ST2 cells was confirmed by Western blotting on day 6 of adipocyte differentiation (Fig. 5*A*).

Surprisingly, ST2 cells overexpressing FAM57B variants 1 and 2 exhibited strongly decreased Oil Red O staining (Fig. 5*B*). This staining pattern was also observed using FLAG-tagged var1F and var2F FAM57B (data not shown). Further analysis demonstrated that the triglyceride content and mRNA expression levels of mature adipocyte markers, notably *Pparγ2*, adiponectin (*AdipoQ*), perilipin 1 (*Plin1*), and glucose transporter 4 (*Glut4*), were all decreased (Fig. 5, *C* and *D*). Overexpressing variant 3 (var3 and var3F) did not result in significant changes in the triglyceride content, Oil Red O staining, or expression level of mature adipocyte markers (Fig. 5, *B–D*).

Next, we knocked down *Fam57b* using three sets of siRNAs (A, B, and C) targeting a common sequence within the *Fam57b* variants (Fig. 1*B*). As shown in Fig. 6*A*, the knockdown efficiency of each siRNA varied from ~70 to 90% on day 2 post-transfection. The Oil Red O staining was slightly increased in ST2 cells treated with each *Fam57b* siRNA compared with the negative control (Fig. 6*B*). We further confirmed that the triglyceride content (Fig. 6*C*) and the expression of adipocyte markers *Pparγ2*, *AdipoQ*, *Plin1* (also a lipid droplet marker), and *Glut4* were all up-regulated (Fig. 6*D*).

Overexpressing FAM57B Augments the Total Ceramide Content in ST2 Cells—FAM57B variants have a TLC domain that is related to ceramide synthase. On the one hand, it is reported that C6-ceramide inhibits adipogenesis using D1 cells (49); here, we confirmed that C6-ceramide also inhibited adipogenesis in ST2 cells (Fig. 7, *A* and *B*). Because overexpressing FAM57B variants 1 and 2 suppressed adipogenesis, we hypothesized that FAM57B could be involved in ceramide synthesis. To evaluate this hypothesis, we analyzed the ceramide content of ST2 cells that were differentiated into adipocytes with each FAM57B variant overexpression. As expected, overexpressing variants 1 and 2, but not variant 3, resulted in an increase in the total ceramide levels (Fig. 7*C*). siRNA-mediated knockdown of *Fam57b*, however, did not decrease the ceramide content (Fig. 7*D*, *left panel*). We considered that this is because other ceramide synthases, such as CERS isoforms 1–6, could function in a compensatory manner to maintain constant ceramide levels. We confirmed that the mRNA expression levels of *Cers2*, *-4*, *-5*, and *-6* (*Cers* isoforms that were detectable in ST2 cells) were significantly increased by si*Fam57b* (Fig. 7*E*). Therefore, we repeated the knockdown experiment using FB1, an inhibitor of ceramide synthase, to reduce the effects of other CERS isoforms. FB1 was added 5 days after si*Fam57b* treatment and the induction of adipogenesis, and the ceramide levels were measured on day 6. As expected, the addition of FB1 decreased the ceramide levels with si*Fam57b* treatment (Fig. 7*D*), indicating that FAM57B has ceramide synthesis activity.

FAM57B Has Ceramide Synthase Activity—We first examined if the increase in ceramide by overexpressing each of the FAM57B variants attributed to the increase in *Cers* or increased sphingomyelinase activity.

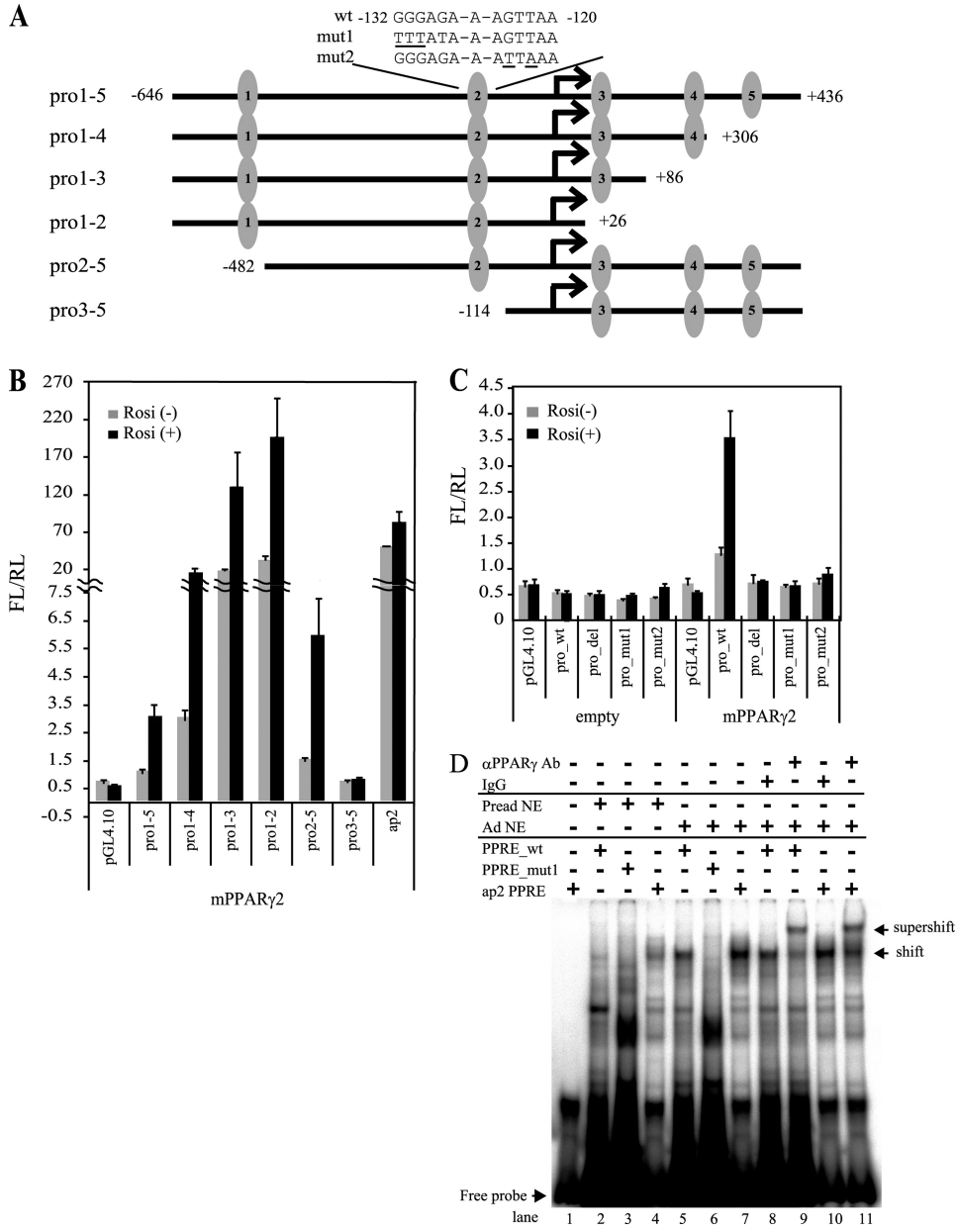

FIGURE 4. **PPARγ binds and activates the gene promoter of *Fam57b* variant 2.** *A*, schematic illustration of *Fam57b* variant 2 promoter and luciferase reporter construct. The five candidates for the PPRE are *numbered 1–5* in the promoter region of *Fam57b* variant 2. These promoter sequences were inserted into the pGL4.10 promoterless reporter vector. The sequences of WT and mutant types (mut1 and mut2) for the second PPRE are indicated. *B*, NIH3T3 cells were transfected with the reporter vectors together with PPARγ or the control expression vector and treated with rosiglitazone (*Rosi*) at 24 h post-transfection for another 24 h. The cells were harvested, and luciferase activity was measured with ARVO according to the manufacturer's instructions. The luciferase activity was shown as FL/RL. FL, firefly luciferase activity was normalized by RL, renilla luciferase. *C*, the pro1–5 wild type (*pro_wt*), pro1–5 mutants 1 and 2 (pro_mut1 and pro_mut2), and pro1–5 PPRE2 deleted (pro_del) were analyzed as described above. *D*, EMSA was performed using a ^{32}P-labeled oligonucleotide containing the above second PPRE WT and mut1 of *Fam57b var2* promoter and *ap2* PPRE as a positive control. The labeled probes were incubated with nuclear extracts of adipocytes (*Ad NE*) and preadipocytes (*Pread NE*) of ST2 cells as a negative control. For the supershift assay, the adipocyte nuclear extract was preincubated with labeled WT or *ap2* PPRE and then incubated with an anti-PPARγ antibody or mouse IgG for 20 min. The DNA-protein complexes were resolved by PAGE. *Lane 1*, free probe; *lanes 2–4*, WT, mut1, and *ap2* PPRE with preadipocyte nuclear extract, respectively; *lanes 5–7*, WT, mut1, and *ap2* PPRE with adipocyte nuclear extract, respectively; *lanes 8* and *10*, WT and *ap2* with mouse IgG and Ad NE, respectively; *lanes 9* and *11*, WT and *ap2* PPRE with PPARγ-specific antibody and adipocyte nuclear extract, respectively. Results are means ± S.D. (*error bars*) ($n = 3$).

There were no differences in the mRNA levels of *Cers* isoform 2, 5 or 6, although *Cers*4 mRNA was down-regulated, in ST2 cells overexpressing each FAM57B variant compared with the control (Fig. 8*A*). There were also no differences in the total sphingomyelinase activity (Fig. 8*B*). Therefore, we further examined if the FAM57B protein has ceramide synthase activity. *In vitro* ceramide synthesis was assessed using fatty acyl-CoA with different acyl chain lengths, including C16, C18, C20, and C22, as substrates. We used CERS2 as a positive control, which uses mainly C20, C22, and C24 as substrates. The ceramide synthase assay using extracts of ST2 cells overexpressing each FAM57B variant (var1, -2, and -3) showed that overexpression of FAM57B variant 2 markedly increased the amount of C16-, C18-, and C20-ceramides compared with the control (Fig. 9*A*).

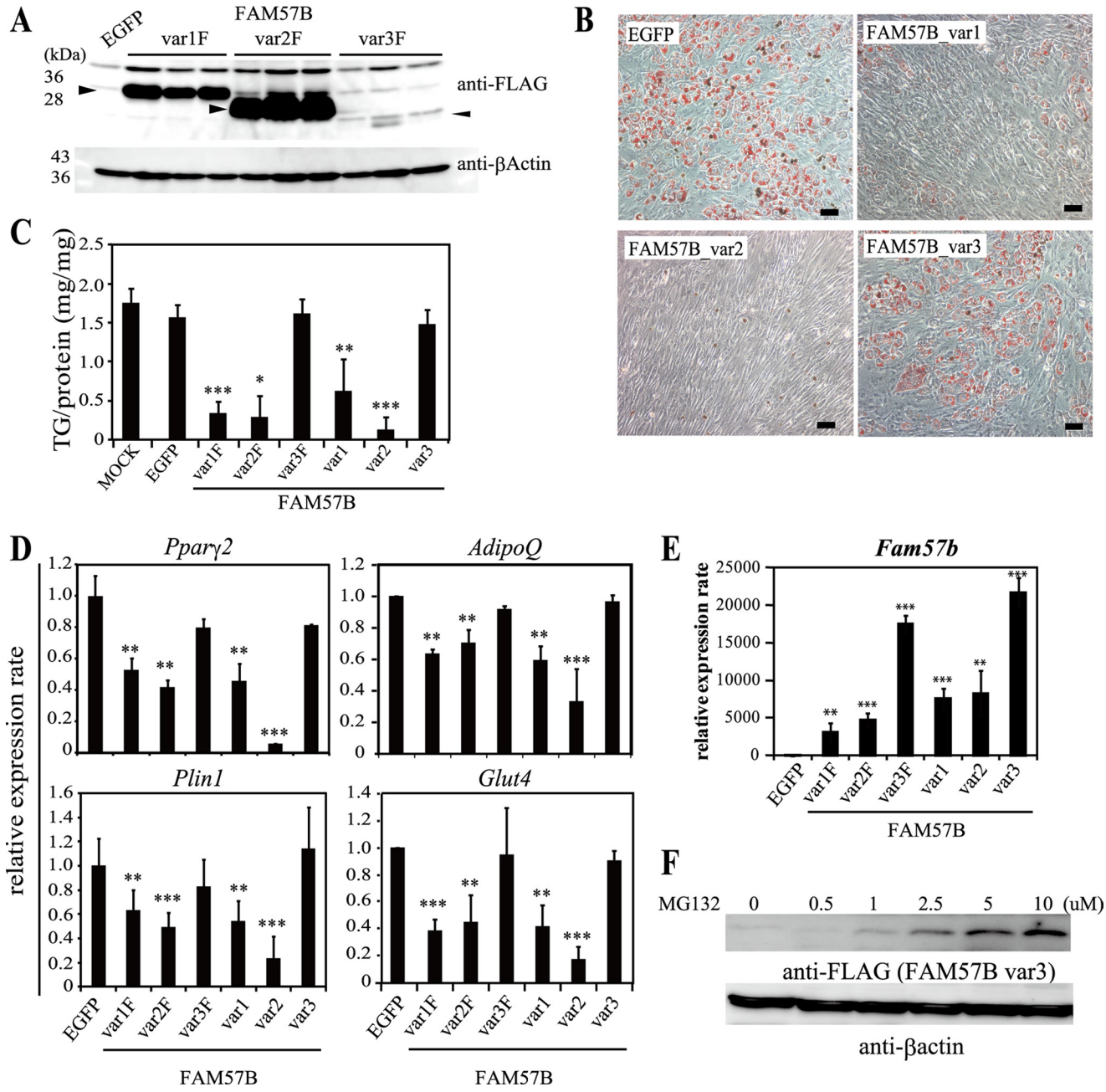

FIGURE 5. **Adipocyte differentiation of ST2 cells is inhibited by overexpression of FAM57B.** *A*, ST2 cells overexpressing FAM57B-FLAG were analyzed on day 6 of adipocyte differentiation by Western blotting using an anti-FLAG antibody. *B*, ST2 cells were infected with retroviruses expressing three different FAM57B variants. Three days after infection, adipogenesis was induced by replacing the medium with fresh medium containing an adipogenic mixture as indicated under "Experimental Procedures." On day 6 of differentiation, the cells were fixed and stained with Oil Red O in which lipids are stained red, at a magnification of ×10. *Scale bar*, 100 μm. *C*, triglyceride (*TG*) content of ST2 cells expressing the FAM57B variants was analyzed on day 6 of adipogenesis. *D*, mRNA level of adipocyte markers was analyzed by qRT-PCR. *E*, we measured the *Fam57b* mRNA levels in ST2 cells overexpressing each FAM57B variant. *F*, ST2 cells overexpressing FAM57B var3 were treated with MG132 at the indicated concentrations for 6–12 h. The cells were harvested and subjected to Western blot analysis using anti-FLAG and anti-β-actin antibodies. Results are means ± S.D. (*error bars*) ($n = 3$); *, $p < 0.05$; **, $p < 0.01$; ***, $p < 0.001$.

We further determined if ceramide synthase activity was blocked with fumonisin B1 using ST2 or 293FT cells that overexpress each variant of FAM57B (Fig. 9, *B* and *C*). As shown in Fig. 9*B*, FAM57B variants 1 and 2 (var1F and var2F) as well as CERS2 augmented the ceramide levels, and this augmentation was inhibited by fumonisin B1, indicating that FAM57B (at least variants 1 and 2) has ceramide synthase activity.

We purified each FAM57B-FLAG variant and CERS2-FLAG to further confirm if FAM57B has ceramide synthase activity. The identity of the purified protein was confirmed by Western blotting as shown in Fig. 9*D*. As shown in Fig. 9*E*, FAM57B variant 2 (var2F) drastically increased the levels of C16-, C18-, and C20-ceramides. Variant 1 (var1F) slightly increased the levels of C18- and C20-ceramides, and variant 3 (var3F) only minimally increased these ceramides.

Ceramide Inhibits Adipogenesis—The variant-specific control of FAM57B in the synthesis of ceramides contributed to the blockade of adipogenesis. These results prompted us to analyze whether

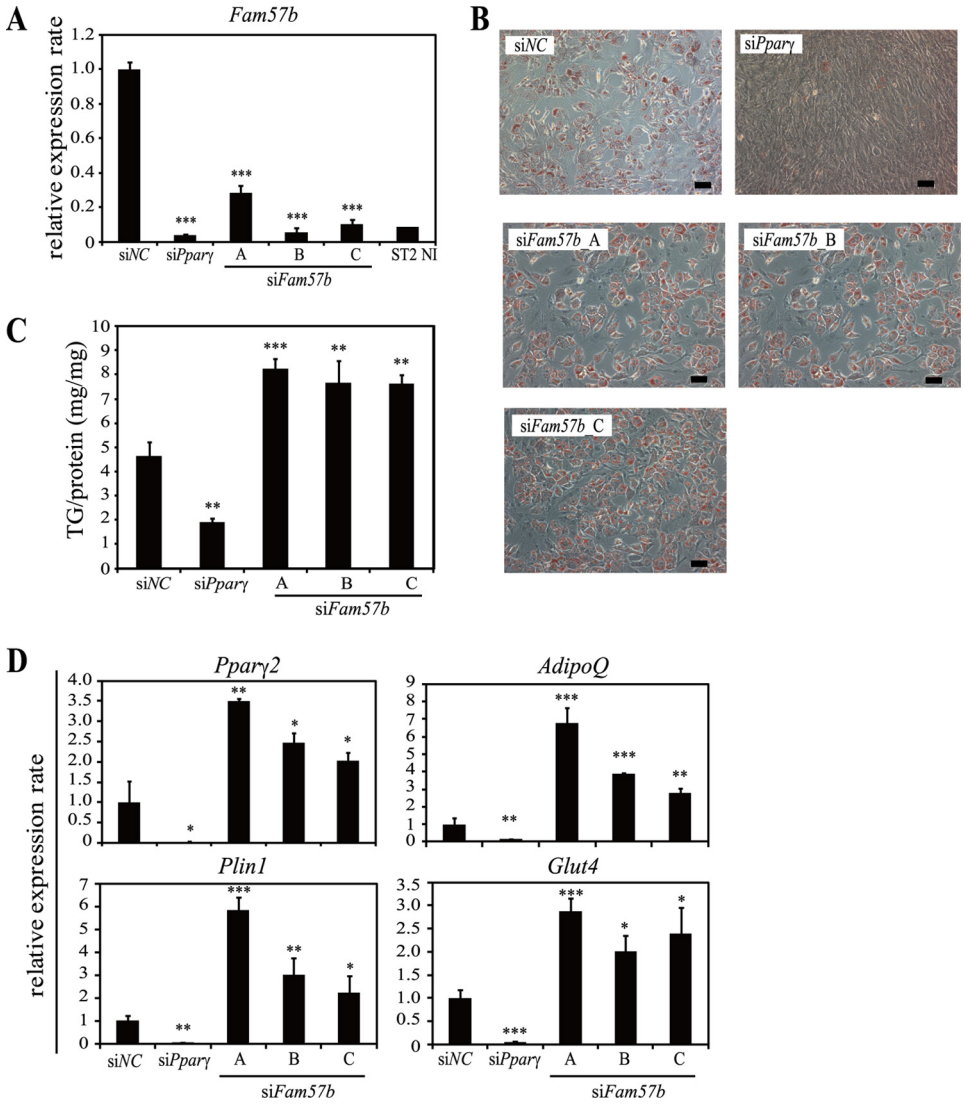

FIGURE 6. **Adipogenic differentiation is promoted by *Fam57b* down-regulation in ST2 cells.** *A*, ST2 cells were transfected with three classes of *Fam57b* siRNA (si*Fam57b*-A, -B, and -C) targeting a common site in all of the *Fam57b* variants. Non-targeting control siRNA (si*NC*) and *Pparγ* siRNA (si*Pparγ*) were used as a negative and positive control, respectively. At 6 h post-transfection, adipogenesis was induced, and total RNA was extracted from the cells on day 2. The knockdown efficiency on day 2 of differentiation was analyzed by real-time RT-PCR. *B*, ST2 cells were treated with siRNA and adipogenic induction and then fixed and stained with Oil Red O on day 6. Magnification was ×10. *Scale bar*, indicates 100 μm. *C*, the triglyceride (*TG*) content was analyzed on day 6 of differentiation. *D*, markers of adipocyte differentiation were analyzed on day 6 of differentiation by qRT-PCR. *Pparγ*, *AdipoQ* and *Glut4* were used as mature adipocyte markers, and perilipin 1 (*Plin1*) was used as a lipid droplet marker. Results are means ± S.D. (*error bars*) ($n = 3$); *, $p < 0.05$; **, $p < 0.01$; ***, $p < 0.001$.

C18- or C20-ceramides could inhibit adipogenesis. As shown in Fig. 10, adipogenesis was inhibited by treating ST2 cells with C18- or C20-ceramides. A statistical analysis showed a significant reduction in adipogenesis and triglyceride levels upon the addition of each ceramide in a dose-dependent manner (Fig. 10, *B* and *C*), indicating the possible involvement of FAM57B in adipogenesis mediated by ceramide production.

DISCUSSION

In this study, we performed an *in vitro* functional analysis of a novel gene, *Fam57b*, that was identified as a PPARγ target gene and involved in obesity by an integrated analysis of three data sets: adipose tissue of HFD/CD, ST2 adipocytes, and *Pparγ* knockdown ST2 cells. Interestingly, FAM57B consists of three variants and has a TLC domain that is related to ceramide synthase. Because ceramide metabolism is dysregulated and augmented in the plasma during obesity and is related to insulin resistance (50, 51), we analyzed the relationship between FAM57B and ceramide and the effects of FAM57B on adipogenesis. We demonstrated that only FAM57B variant 2 is directly targeted by PPARγ and could regulate adipogenesis through ceramide metabolism.

Fam57b variant 2 was up-regulated during adipogenesis and by rosiglitazone treatment (Fig. 2, *A* and *C*). The variant 2 was up-regulated slowly starting on day 2 until day 6 and then down-regulated on day 10 (Fig. 2, *A* and *B*) (data not shown). These results suggested that the appropriate timing of *Fam57b* expression is important in adipogenesis.

We demonstrated that *Fam57b* variant 2 is a direct target of PPARγ by ChIP-qPCR (Fig. 3*B*), reporter assay (Fig. 4, *B* and *C*), and EMSA (Fig. 4*D*). In the ChIP-qPCR assay, the PCR product

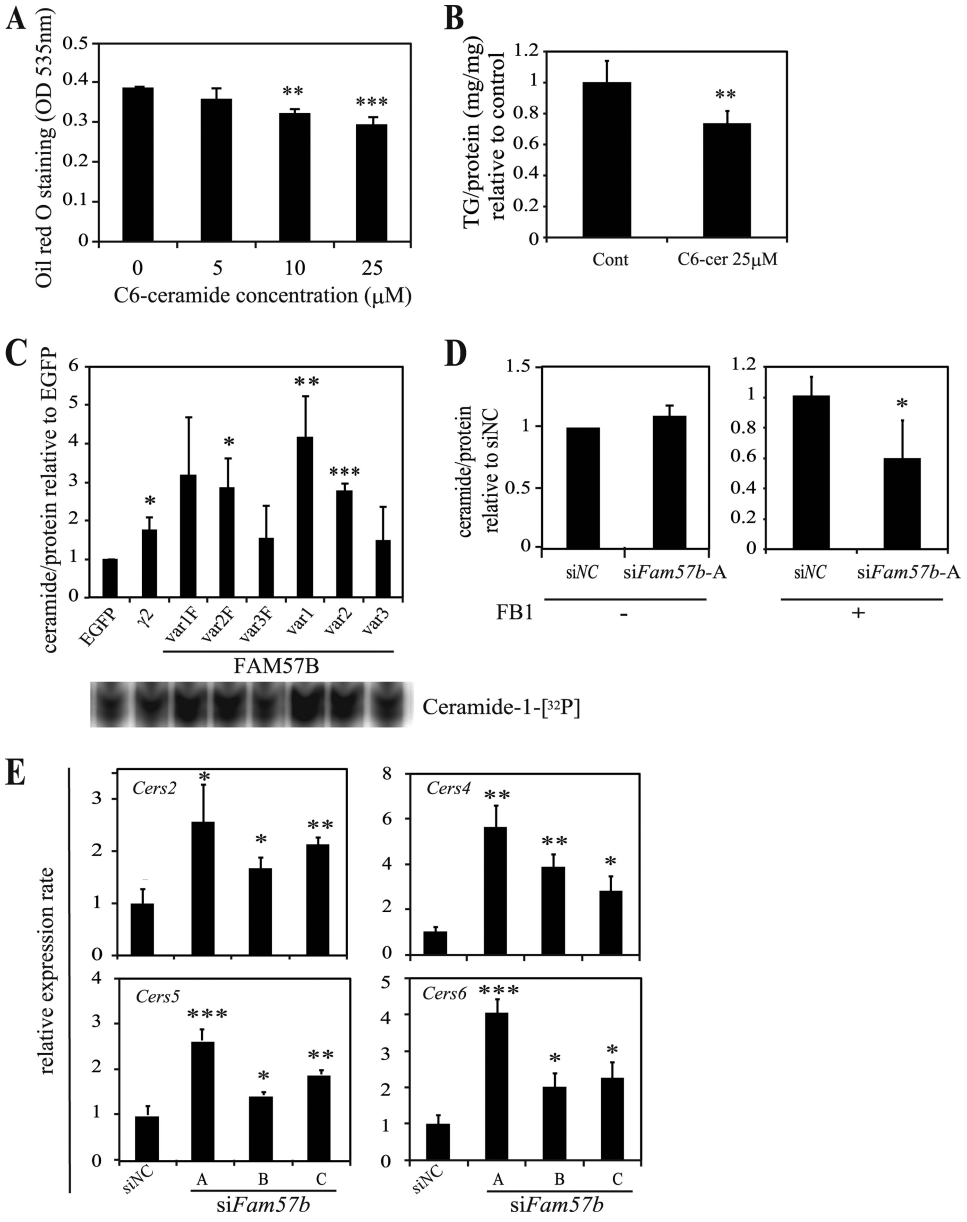

FIGURE 7. **Total ceramide content is augmented in ST2 cells overexpressing FAM57B.** *A*, ST2 cells were treated with the indicated concentration of C6-ceramide during adipogenesis and then stained with Oil Red O on day 6 of differentiation. The Oil Red O that accumulated in lipid droplets was extracted with isopropyl alcohol and measured at OD 535 nm. *B*, the triglyceride content was measured on day 6 of adipogenesis and is presented as the triglyceride levels normalized to the protein levels and the control. *C*, ST2 cells overexpressing each FAM57B variant with (*var1F–var3F*) and without FLAG (*var1–var3*) were differentiated into adipocytes for 6 days. Total lipids were extracted from cell lysates containing 200 μg of protein and subjected to the diacylglycerol kinase assay that enzymatically phosphorylates and labels lipids with ^{32}P (*Ceramide-1-[^{32}P]*), as described under "Experimental Procedures." The samples were spotted onto thin layer chromatography plates and developed in organic solvents (*bottom panel*). The ceramide levels were digitized by measuring the band intensity with an Image analyzer (Image Gauge version 3.4, FUJIFILM), normalized to the protein levels, and then expressed relative to the control (EGFP-expressing cells). γ*2* represents the ceramide levels that accumulated upon PPARγ overexpression as a positive control. The experiment was performed at least three times. *D*, the ceramide content of si*Fam57b*-A treated ST2 cells was examined in a similar manner with or without 20 μM FB1, a ceramide synthase inhibitor, which was added from day 5 to 6 of differentiation. The ceramide levels were measured 6 days after differentiation using 100 μg of protein. The relative ceramide levels between si*NC* and si*Fam57b* are shown for both conditions with and without FB1. *E*, ST2 cells were treated with siRNA (si*NC* and si*Fam57b*-A, -B, and -C) and induced to undergo adipogenesis. On day 6, total RNA was extracted and analyzed by qRT-PCR. The mRNA expression of *Cers2*, *-4*, *-5*, and *-6* was measured using the primer sets listed in Table 2. Results are means ± S.D. (*error bars*) for three individual experiments. *, $p < 0.05$; **, $p < 0.01$; ***, $p < 0.001$.

of the variant 2 promoter sequence was significantly concentrated by an anti-PPARγ antibody, whereas that of variants 1 and 3 was less concentrated (Fig. 3*B*), indicating that the putative PPRE of the variant 2 promoter is the major target of PPARγ. Based on a reporter assay, the specific region of the variant 2 promoter was also identified as PPRE, and direct binding of PPARγ to this specific target sequence was further confirmed by EMSA (Fig. 4*D*). Interestingly, higher luciferase activity was observed when the downstream region of the transcription start site of *Fam57b* variant 2 was deleted, suggesting that the expression of *Fam57b* variant 2 could be negatively regulated by this region.

Although variant 2 is a direct target of PPARγ, the restricted expression at later stages of adipogenesis awaits further clarification. Variants 1 and 3 were also up-regulated during adipogenesis to a different degree compared with var-

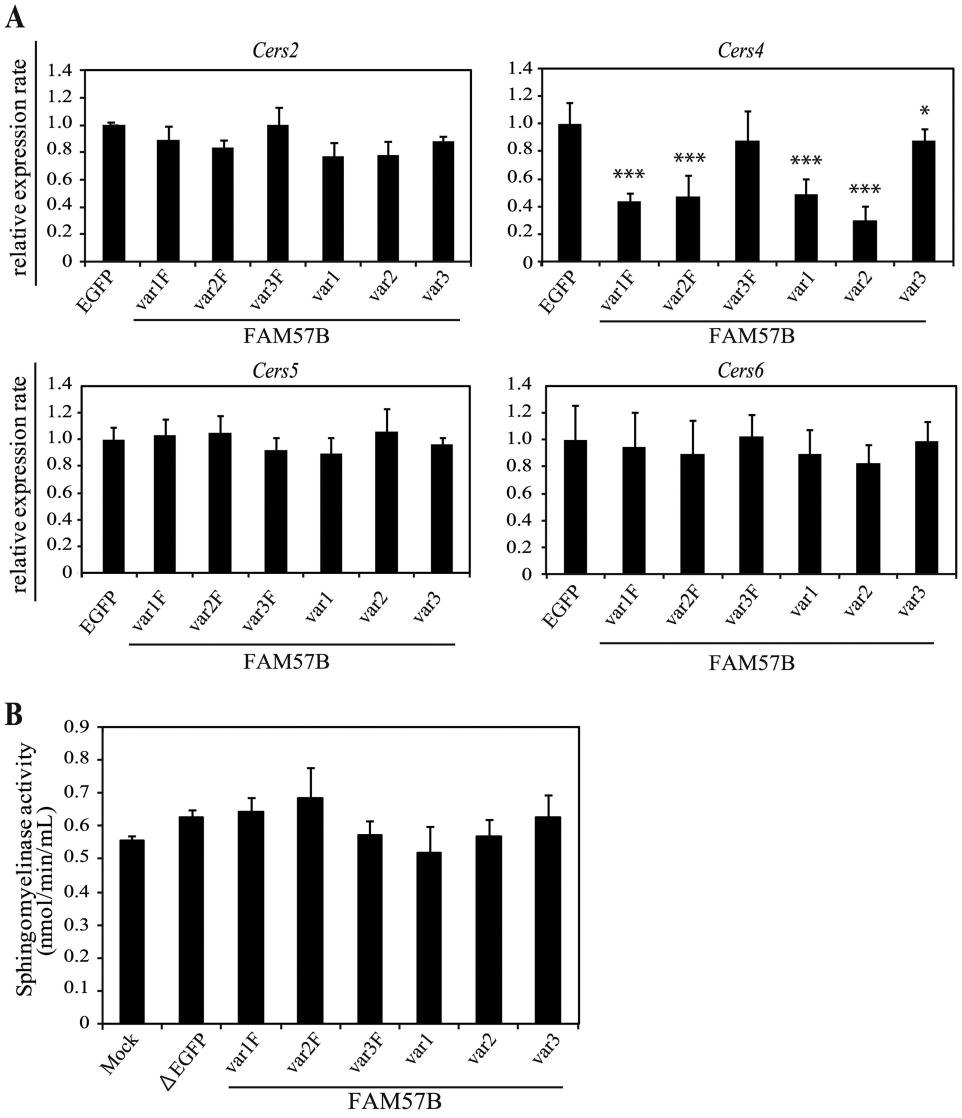

FIGURE 8. **FAM57B overexpression does not affect the mRNA expression levels of ceramide synthase or sphingomyelinase activity.** *A*, the mRNA expression levels of four ceramide synthases (*Cers2*, *-4*, *-5*, and *-6*) in differentiated FAM57B-overexpressing ST2 cells on day 6 were analyzed by qRT-PCR. *B*, the total sphingomyelinase activity was analyzed in differentiated FAM57B-overexpressing ST2 cells on day 6 using a sphingomyelinase assay kit. Results are means ± S.D. (*error bars*) for three individual experiments. *, $p < 0.05$; **, $p < 0.01$; ***, $p < 0.001$.

iant 2 (*i.e.* variant 1 was up-regulated more slowly than variant 2, and variant 3 was relatively low throughout adipogenesis). The expression of variant 1 reached the same level at day 6 after adipogenic induction (Fig. 2*A*). However, *Fam57b* variant 1 is unlikely to be regulated by PPARγ (Fig. 2*C*) but rather by other transcription factors related to adipogenesis. Alternatively, we cannot rule out the possibility that PPARγ might be involved in the expression of variants 1 and 3 in the distal region of the *Fam57b* gene promoter along with other transcription factors. Further investigation is required to elucidate the roles of these factors.

When tissue expression was analyzed, there was a distinct expression profile among the three variants in which variant 1 was up-regulated mainly in the brain, whereas variant 2 was expressed in the testis and adipose tissue and variant 3 was only weakly expressed in all tissues (Fig. 2*D*). This tissue-specific expression could indicate that each variant has important roles in individual tissues.

The role of each FAM57B variant in adipogenesis was demonstrated using overexpression and siRNA knockdown assays. Variants 1 and 2 inhibited adipogenesis, whereas variant 3 had little effect on adipogenesis. The differential effects of the three variants might reflect the expression level of each variant, in which the protein expression of variant 2 was the highest, whereas variant 3 was the lowest, although the mRNA levels of overexpressed variants 1, 2, and 3 were comparably high (Fig. 5*E*). The protein level of variant 3 was recovered by treating with the proteasome inhibitor MG132 (Fig. 5*F*). Therefore, the reduced effects of FAM57B variant 3 on adipogenesis could be explained by the reduced expression of variant 3 as a result of protein degradation. These results suggest that variants 1 and 2 have roles in regulating adipogenesis.

The ability of FAM57B variant 2 to inhibit adipogenesis could be explained by the augmented ceramides that we attributed to this variant. Indeed, we demonstrated that C6-, C18-, or C20-ceramides inhibited the adipogenesis of ST2 cells (Figs. 7,

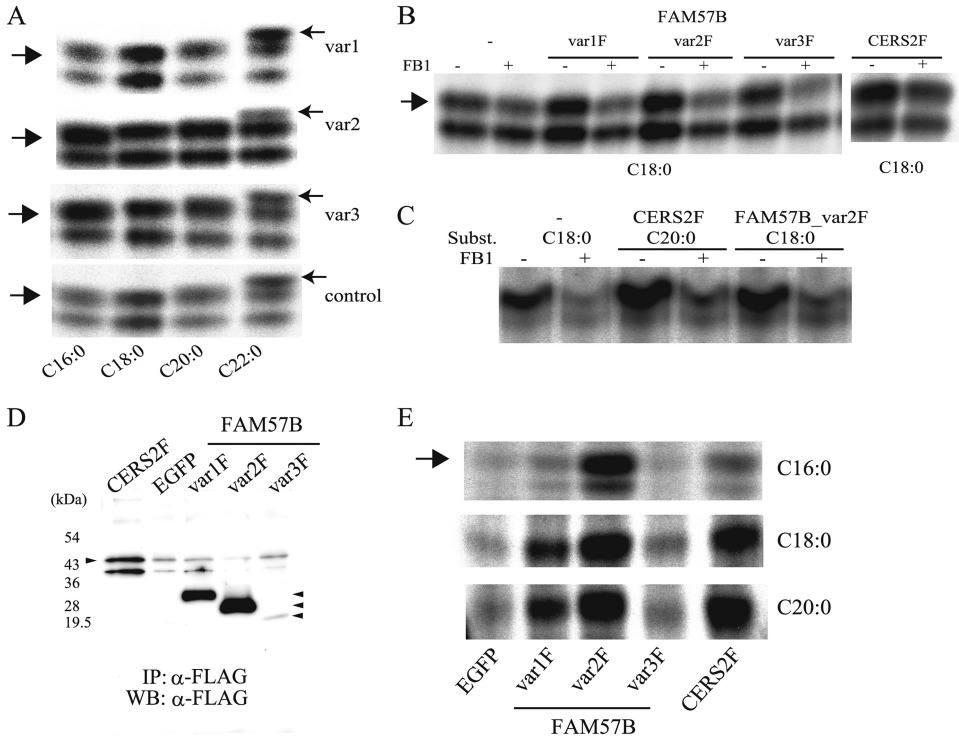

FIGURE 9. **Ceramide synthase activity of the FAM57B protein.** *A*, *in vitro* ceramide synthase activity was measured using differentiated ST2 cell extracts (50 μg of protein), which overexpressed each FAM57B variant (*var1–var3*) with different substrates, such as palmitoyl-CoA (C16:0), stearoyl-CoA (C18:0), arachidoyl-CoA (C20:0), and behenoyl-CoA (C22:0). *B*, an *in vitro* ceramide synthase assay was performed using undifferentiated FAM57B-FLAG or ceramide synthase 2-FLAG (CERS2F)-overexpressed ST2 cell extracts (50 μg of protein) that were preincubated with or without 20 μM FB1, followed by adding C18-acyl-CoA as substrate. *C*, *in vitro* ceramide synthase activity with or without fumonisin B1 was assayed using 293FT cell extracts (50 μg of protein), which transiently overexpressed FAM57B var2F or CERS2F. *D*, ST2 cells overexpressing CERS2F, EGFP, or FAM57B-F (each variant) were immunoprecipitated (*IP*) with an anti-FLAG antibody, which was released with 3× FLAG peptide, and subjected to Western blot analysis (*WB*) using an anti-FLAG antibody. *E*, *in vitro* ceramide synthase activity was measured using purified FAM57B-FLAG protein (var1F–var3F) and CERS2F, with different substrates, such as C16-, C18- and C20-acyl-CoA. Results are representative of three independent experiments.

A and *B*, and 10). This phenomenon is also consistent with previous reports that C6-ceramide treatment inhibited adipogenesis in D1 murine mesenchymal stem cells (49). On the other hand, ceramide levels reportedly decrease with adipogenesis (52), and we have reproduced this phenomenon in ST2 cells (data not shown), suggesting that the decrease in ceramide levels is necessary during adipogenesis.

Because FAM57B has a TLC domain and overexpression of FAM57B augmented ceramide levels, we hypothesized that FAM57B variant 2 acts as a ceramide synthase. Although variant 2 does not show high homology to classic ceramide synthase (CERS), we demonstrated experimentally using FAM57B variant 2-overexpressing cells and purified FAM57B protein that variant 2 augmented ceramides *in vitro*. Thus, we concluded that FAM57B variant 2 plays a role in *de novo* synthesis of ceramide.

Variant 1 also has ceramide synthase activity. Indeed, variant 1 inhibited adipogenesis, augmented ceramide levels, and exhibited ceramide synthase activity *in vitro* using ST2 cell extracts overexpressing variant 1 and with purified protein. The preference of substrates is probably different between variant 1 and variant 2. Variant 2 uses C16, C18, and C20, whereas variant 1 uses C18 and C20 but not C16 acyl-CoA. On the other hand, variant 3 had little effect on adipogenesis, and the ceramide content did not apparently change with ST2 cell extracts overexpressing variant 3 and in purified protein. This relatively low effect may be attributed to protein instability.

Although *Fam57b* is a regulatory target of PPARγ, *Pparγ2* expression was decreased upon FAM57B overexpression (Fig. 5*D*), suggesting that FAM57B acts as a negative feedback factor. In fact, the idea is strikingly supported by the significant augmentation of *Pparγ2* gene expression as well as that of other adipogenesis markers by knocking down *Fam57b* (Fig. 6*D*). Because the FAM57B protein is distributed in the ER and Golgi (data not shown), it is unlikely that FAM57B directly inhibits the expression of PPARγ. However, a previous report showed that C2-ceramide inhibited adipogenesis by decreasing the transcriptional activity of C/EBPβ and PPARγ expression (53). Hence, we thought that PPARγ expression was decreased through FAM57B-mediated regulation of ceramides.

Because FAM57B overexpression resulted in an increase in ceramides followed by an inhibition of adipogenesis, we speculate that the decrease in ceramides upon FAM57B knockdown could promote adipogenesis. As expected, adipogenesis was promoted by knocking down FAM57B; however, unexpectedly the total ceramide levels did not decrease, probably due to the compensation of ceramides by other ceramide synthases (Fig. 7*E*). Because ceramides have a sphingolipid backbone and are metabolized to biologically active substances, such as sphingosine 1-phosphate, which can promote adipogenesis (54), ceramides are thought to serve as precursors for other bioactive sphingolipids. Altogether, we conclude that ceramides are important for adipogenesis. However, excess ceramides inhibit adipogenesis, indicating that ceramide levels should be tightly

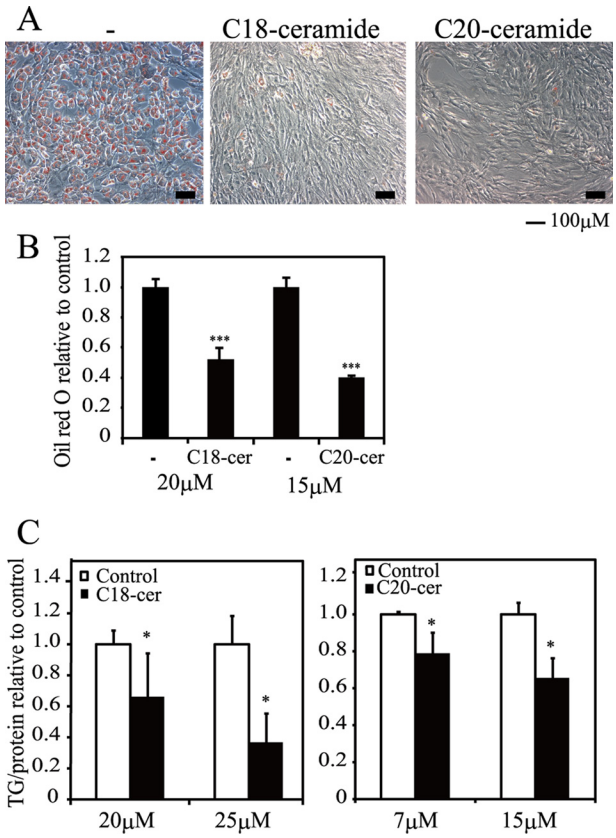

FIGURE 10. **Effect of C18- and C20-ceramide on ST2 adipogenesis.** *A*, ST2 cells were treated with 20 μM C18-ceramide (*C18-cer*), or 15 μM C20-ceramide (*C20-cer*) during adipogenesis. The cells were stained with Oil Red O on day 6 of differentiation. *Scale bar*, 100 μm. *B*, the Oil Red O, which accumulated in lipid droplets, was extracted with isopropyl alcohol and measured at OD 535 nm. *C*, ST2 cells were treated with 20 or 25 μM C18-ceramide and 7 μM or 15 μM C20-ceramide during adipogenesis. The relative triglyceride levels were measured on day 6 of differentiation and normalized to the total protein levels. *, $p < 0.05$; **, $p < 0.01$; ***, $p < 0.001$. *Error bars*, S.D.

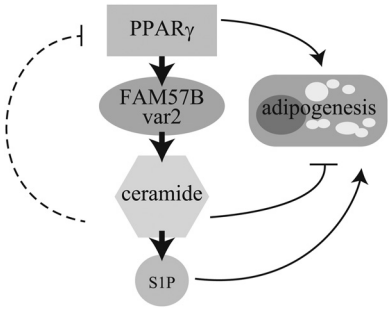

FIGURE 11. **The proposed role of FAM57B in adipogenesis.** PPARγ directly controls FAM57B var2 expression, and consequently FAM57B synthesizes ceramides during adipogenesis. PPARγ is the master regulator of adipogenesis. FAM57B also regulates adipogenesis through ceramide metabolism. High ceramide levels could inhibit adipogenesis, whereas low levels might promote adipogenesis by being converted to sphingosin 1-phosphate (*S1P*), which is another sphingolipid that promotes adipogenesis and generally works contrary to ceramides.

regulated, and FAM57B could play a role in this fine-tuned regulation (Fig. 11).

Recent evidence demonstrated that sphingolipid metabolism is dysregulated in obesity (50, 51). Pharmacological and genetic approaches have shown that decreased ceramide synthesis results in improved insulin sensitivity in rodent models of insulin resistance (54). These authors hypothesized that ceramide generated and secreted from visceral adipose tissue could contribute to insulin resistance in the liver and muscle. Our findings also showed that *Fam57b* variant 2 is up-regulated in obese adipose tissue (Fig. 2*E*). This increased expression may contribute in part to the augmented ceramide levels in adipose tissue and subsequently to insulin resistance. On the other hand, *Fam57b* variants 1 and 3 were down-regulated in obese adipose tissue. Therefore, the function of these variants in obesity is probably different from that of variant 2. Thus, it would be interesting to further analyze the relationship between FAM57B and ceramides in obese adipose tissues. The mechanism by which variant 2 is up-regulated in obese adipose tissue also remains to be clarified. Recently, it was reported that PPARγ phosphorylation increases in obese adipose tissue, resulting in the up-regulation of lipid metabolism-related genes (55). *Fam57b* variant 2 might also be regulated by phosphorylated PPARγ. As another possibility, a transcription factor, such as NF-κB, that is induced in obese tissue due to inflammation might contribute to the up-regulation because NF-κB-binding sites were identified in the promoter region of *Fam57b* variant 2 using an *in silico* analysis.

In conclusion, we demonstrated that a novel PPARγ target gene, *Fam57b* variant 2, regulates adipocyte differentiation with ceramide as an effector (Fig. 11). Our findings suggested a new pathway of PPARγ-mediated ceramide metabolism and may offer new therapeutic targets for obesity or metabolic syndrome.

Acknowledgments—We thank Masafumi Onodera for providing the retroviral vector and Toshio Kitamura for providing Plat-E cells. We greatly appreciate the technical assistance of Mioko Iseki and are grateful to Yuichi Ninomiya and Hiroyoshi Iseki for critical suggestions for the experiments. We thank Toshiwo Andoh for critically reading the manuscript and all members of the laboratory for suggestions and advice in writing the manuscript.

REFERENCES

1. Bonora, E., Brangani, C., and Pichiri, I. (2008) [Abdominal obesity and diabetes]. *G. Ital. Cardiol.* **9,** 40S–53S
2. Després, J. P., and Lemieux, I. (2006) Abdominal obesity and metabolic syndrome. *Nature* **444,** 881–887
3. Hotamisligil, G. S., Shargill, N. S., and Spiegelman, B. M. (1993) Adipose expression of tumor necrosis factor-α. Direct role in obesity-linked insulin resistance. *Science* **259,** 87–91
4. Gerhardt, C. C., Romero, I. A., Cancello, R., Camoin, L., and Strosberg, A. D. (2001) Chemokines control fat accumulation and leptin secretion by cultured human adipocytes. *Mol. Cell. Endocrinol.* **175,** 81–92
5. Sartipy, P., and Loskutoff, D. J. (2003) Monocyte chemoattractant protein 1 in obesity and insulin resistance. *Proc. Natl. Acad. Sci. U.S.A.* **100,** 7265–7270
6. Hutley, L., and Prins, J. B. (2005) Fat as an endocrine organ. Relationship to the metabolic syndrome. *Am. J. Med. Sci.* **330,** 280–289
7. Fried, S. K., Bunkin, D. A., and Greenberg, A. S. (1998) Omental and subcutaneous adipose tissues of obese subjects release interleukin-6. Depot difference and regulation by glucocorticoid. *J. Clin. Endocrinol. Metab.* **83,** 847–850
8. Ozel Demiralp, D., Aktas, H., and Akar, N. (2008) The effect of plasminogen activator inhibitor-1–675 4G/5G polymorphism on PAI-1 gene expression and adipocyte differentiation. *Clin. Appl. Thromb. Hemost.* **14,** 438–446
9. Tontonoz, P., Hu, E., Graves, R. A., Budavari, A. I., and Spiegelman, B. M.

(1994) mPPAR γ 2. Tissue-specific regulator of an adipocyte enhancer. *Genes Dev.* **8,** 1224–1234
10. Tontonoz, P., Hu, E., and Spiegelman, B. M. (1994) Stimulation of adipogenesis in fibroblasts by PPAR γ 2, a lipid-activated transcription factor. *Cell* **79,** 1147–1156
11. Chawla, A., Schwarz, E. J., Dimaculangan, D. D., and Lazar, M. A. (1994) Peroxisome proliferator-activated receptor (PPAR) γ. Adipose-predominant expression and induction early in adipocyte differentiation. *Endocrinology* **135,** 798–800
12. Gray, S. L., Dalla Nora, E., and Vidal-Puig, A. J. (2005) Mouse models of PPAR-γ deficiency. Dissecting PPAR-γ's role in metabolic homoeostasis. *Biochem. Soc. Trans.* **33,** 1053–1058
13. Lehmann, J. M. (1995) An antidiabetic thiazolidinedione is a high affinity ligand for peroxisome proliferator-activated receptor γ (PPARγ). *J. Biol. Chem.* **270,** 12953–12956
14. Sharma, A. M., and Staels, B. (2007) Review. Peroxisome proliferator-activated receptor γ and adipose tissue. Understanding obesity-related changes in regulation of lipid and glucose metabolism. *J. Clin. Endocrinol. Metab.* **92,** 386–395
15. Trujillo, M. E., and Scherer, P. E. (2006) Adipose tissue-derived factors. Impact on health and disease. *Endocr. Rev.* **27,** 762–778
16. Lipscombe, L. L., Gomes, T., Lévesque, L. E., Hux, J. E., Juurlink, D. N., and Alter, D. A. (2007) Thiazolidinediones and cardiovascular outcomes in older patients with diabetes. *JAMA* **298,** 2634–2643
17. Schorling, S., Vallée, B., Barz, W. P., Riezman, H., and Oesterhelt, D. (2001) Lag1p and Lac1p are essential for the Acyl-CoA-dependent ceramide synthase reaction in *Saccharomyces cerevisae*. *Mol. Biol. Cell* **12,** 3417–3427
18. Mizutani, Y., Kihara, A., and Igarashi, Y. (2005) Mammalian Lass6 and its related family members regulate synthesis of specific ceramides. *Biochem. J.* **390,** 263–271
19. Venkataraman, K., Riebeling, C., Bodennec, J., Riezman, H., Allegood, J. C., Sullards, M. C., Merrill, A. H., Jr., and Futerman, A. H. (2002) Upstream of growth and differentiation factor 1 (uog1), a mammalian homolog of the yeast longevity assurance gene 1 (LAG1), regulates *N*-stearoyl-sphinganine (C18-(dihydro)ceramide) synthesis in a fumonisin B1-independent manner in mammalian cells. *J. Biol. Chem.* **277,** 35642–35649
20. Riebeling, C., Allegood, J. C., Wang, E., Merrill, A. H., Jr., and Futerman, A. H. (2003) Two mammalian longevity assurance gene (LAG1) family members, trh1 and trh4, regulate dihydroceramide synthesis using different fatty acyl-CoA donors. *J. Biol. Chem.* **278,** 43452–43459
21. Mizutani, Y., Kihara, A., and Igarashi, Y. (2006) LASS3 (longevity assurance homologue 3) is a mainly testis-specific (dihydro)ceramide synthase with relatively broad substrate specificity. *Biochem. J.* **398,** 531–538
22. Pan, H., Qin, W. X., Huo, K. K., Wan, D. F., Yu, Y., Xu, Z. G., Hu, Q. D., Gu, K. T., Zhou, X. M., Jiang, H. Q., Zhang, P. P., Huang, Y., Li, Y. Y., and Gu, J. R. (2001) Cloning, mapping, and characterization of a human homologue of the yeast longevity assurance gene LAG1. *Genomics* **77,** 58–64
23. Wang, B., Shi, G., Fu, Y., and Xu, X. (2007) Cloning and characterization of a LASS1-GDF1 transcript in rat cerebral cortex. Conservation of a bicistronic structure. *DNA Seq.* **18,** 92–103
24. Perry, D. K., and Hannun, Y. A. (1998) The role of ceramide in cell signaling. *Biochim. Biophys. Acta* **1436,** 233–243
25. Gulbins, E. (2003) Regulation of death receptor signaling and apoptosis by ceramide. *Pharmacol. Res.* **47,** 393–399
26. Marchesini, N., and Hannun, Y. A. (2004) Acid and neutral sphingomyelinases. Roles and mechanisms of regulation. *Biochem. Cell Biol.* **82,** 27–44
27. Irizarry, R. A., Bolstad, B. M., Collin, F., Cope, L. M., Hobbs, B., and Speed, T. P. (2003) Summaries of Affymetrix GeneChip probe level data. *Nucleic Acids Res.* **31,** e15
28. Mizuno, Y., Yagi, K., Tokuzawa, Y., Kanesaki-Yatsuka, Y., Suda, T., Katagiri, T., Fukuda, T., Maruyama, M., Okuda, A., Amemiya, T., Kondoh, Y., Tashiro, H., and Okazaki, Y. (2008) miR-125b inhibits osteoblastic differentiation by down-regulation of cell proliferation. *Biochem. Biophys. Res. Commun.* **368,** 267–272
29. Morita, S., Kojima, T., and Kitamura, T. (2000) Plat-E. An efficient and stable system for transient packaging of retroviruses. *Gene Ther.* **7,** 1063–1066
30. Chalfant, C. E., Kishikawa, K., Mumby, M. C., Kamibayashi, C., Bielawska, A., and Hannun, Y. A. (1999) Long chain ceramides activate protein phosphatase-1 and protein phosphatase-2A. Activation is stereospecific and regulated by phosphatidic acid. *J. Biol. Chem.* **274,** 20313–20317
31. Wakabayashi, K., Okamura, M., Tsutsumi, S., Nishikawa, N. S., Tanaka, T., Sakakibara, I., Kitakami, J., Ihara, S., Hashimoto, Y., Hamakubo, T., Kodama, T., Aburatani, H., and Sakai, J. (2009) The peroxisome proliferator-activated receptor γ/retinoid X receptor α heterodimer targets the histone modification enzyme PR-Set7/Setd8 gene and regulates adipogenesis through a positive feedback loop. *Mol. Cell. Biol.* **29,** 3544–3555
32. Tomaru, T., Steger, D. J., Lefterova, M. I., Schupp, M., and Lazar, M. A. (2009) Adipocyte-specific expression of murine resistin is mediated by synergism between peroxisome proliferator-activated receptor γ and CCAAT/enhancer-binding proteins. *J. Biol. Chem.* **284,** 6116–6125
33. Tokuzawa, Y., Yagi, K., Yamashita, Y., Nakachi, Y., Nikaido, I., Bono, H., Ninomiya, Y., Kanesaki-Yatsuka, Y., Akita, M., Motegi, H., Wakana, S., Noda, T., Sablitzky, F., Arai, S., Kurokawa, R., Fukuda, T., Katagiri, T., Schönbach, C., Suda, T., Mizuno, Y., and Okazaki, Y. (2010) Id4, a new candidate gene for senile osteoporosis, acts as a molecular switch promoting osteoblast differentiation. *PLoS Genet.* **6,** e1001019
34. Yagi, K., Kondo, D., Okazaki, Y., and Kano, K. (2004) A novel preadipocyte cell line established from mouse adult mature adipocytes. *Biochem. Biophys. Res. Commun.* **321,** 967–974
35. Chavez, J. A., and Summers, S. A. (2003) Characterizing the effects of saturated fatty acids on insulin signaling and ceramide and diacylglycerol accumulation in 3T3-L1 adipocytes and C2C12 myotubes. *Arch. Biochem. Biophys.* **419,** 101–109
36. Kim, J. Y., Tillison, K., Lee, J. H., Rearick, D. A., and Smas, C. M. (2006) The adipose tissue triglyceride lipase ATGL/PNPLA2 is downregulated by insulin and TNF-α in 3T3-L1 adipocytes and is a target for transactivation by PPARγ. *Am. J. Physiol. Endocrinol. Metab.* **291,** E115–E127
37. Nakachi, Y., Yagi, K., Nikaido, I., Bono, H., Tonouchi, M., Schönbach, C., and Okazaki, Y. (2008) Identification of novel PPARγ target genes by integrated analysis of ChIP-on-chip and microarray expression data during adipocyte differentiation. *Biochem. Biophys. Res. Commun.* **372,** 362–366
38. Fiorito, M., Torrente, I., De Cosmo, S., Guida, V., Colosimo, A., Prudente, S., Flex, E., Menghini, R., Miccoli, R., Penno, G., Pellegrini, F., Tassi, V., Federici, M., Trischitta, V., and Dallapiccola, B. (2007) Interaction of DIO2 T92A and PPARγ2 P12A polymorphisms in the modulation of metabolic syndrome. *Obesity* **15,** 2889–2895
39. Christianson, J. L., Nicoloro, S., Straubhaar, J., and Czech, M. P. (2008) Stearoyl-CoA desaturase 2 is required for peroxisome proliferator-activated receptor γ expression and adipogenesis in cultured 3T3-L1 cells. *J. Biol. Chem.* **283,** 2906–2916
40. Neve, E. P., Nordling, A., Andersson, T. B., Hellman, U., Diczfalusy, U., Johansson, I., and Ingelman-Sundberg, M. (2012) Amidoxime reductase system containing cytochrome b_5 type B (CYB5B) and MOSC2 is of importance for lipid synthesis in adipocyte mitochondria. *J. Biol. Chem.* **287,** 6307–6317
41. Xu, L., Mirnics, K., Bowman, A. B., Liu, W., Da, J., Porter, N. A., and Korade, Z. (2012) DHCEO accumulation is a critical mediator of pathophysiology in a Smith-Lemli-Opitz syndrome model. *Neurobiol Dis.* **45,** 923–929
42. Wang, J. L., Ren, Z. Y., Xia, J. B., Huang, S., Qi, M. H., Wang, L. M., and Ye, J. (2011) [The mechanism of airway inflammation in eosinophilic bronchitis and cough variant asthma]. *Zhonghua Jie He He Hu Xi Za Zhi* **34,** 433–437
43. Nair, S., Lee, Y. H., Rousseau, E., Cam, M., Tataranni, P. A., Baier, L. J., Bogardus, C., and Permana, P. A. (2005) Increased expression of inflammation-related genes in cultured preadipocytes/stromal vascular cells from obese compared with non-obese Pima Indians. *Diabetologia* **48,** 1784–1788
44. Horie, M., Okutomi, K., Taniguchi, Y., Ohbuchi, Y., Suzuki, M., and Takahashi, E. (1998) Isolation and characterization of a new member of the human Ly6 gene family (LY6H). *Genomics* **53,** 365–368
45. Poli, M., Luscieti, S., Gandini, V., Maccarinelli, F., Finazzi, D., Silvestri, L., Roetto, A., and Arosio, P. (2010) Transferrin receptor 2 and HFE regulate

furin expression via mitogen-activated protein kinase/extracellular signal-regulated kinase (MAPK/Erk) signaling. Implications for transferrin-dependent hepcidin regulation. *Haematologica* **95,** 1832–1840
46. Hintsch, G., Zurlinden, A., Meskenaite, V., Steuble, M., Fink-Widmer, K., Kinter, J., and Sonderegger, P. (2002) The calsyntenins. A family of postsynaptic membrane proteins with distinct neuronal expression patterns. *Mol. Cell Neurosci.* **21,** 393–409
47. Winter, E., and Ponting, C. P. (2002) TRAM, LAG1 and CLN8. Members of a novel family of lipid-sensing domains?. *Trends. Biochem. Sci.* **27,** 381–383
48. Hirokawa, T., Boon-Chieng, S., and Mitaku, S. (1998) SOSUI. Classification and secondary structure prediction system for membrane proteins. *Bioinformatics* **14,** 378–379
49. Xu, F., Yang, C. C., Gomillion, C., and Burg, K. J. (2010) Effect of ceramide on mesenchymal stem cell differentiation toward adipocytes. *Appl. Biochem. Biotechnol.* **160,** 197–212
50. Yang, G., Badeanlou, L., Bielawski, J., Roberts, A. J., Hannun, Y. A., and Samad, F. (2009) Central role of ceramide biosynthesis in body weight regulation, energy metabolism, and the metabolic syndrome. *Am. J. Physiol. Endocrinol. Metab.* **297,** E211–E224
51. Samad, F., Badeanlou, L., Shah, C., and Yang, G. (2011) Adipose tissue and ceramide biosynthesis in the pathogenesis of obesity. *Adv. Exp. Med. Biol.* **721,** 67–86
52. Choi, K. M., Lee, Y. S., Choi, M. H., Sin, D. M., Lee, S., Ji, S. Y., Lee, M. K., Lee, Y. M., Yun, Y. P., Hong, J. T., and Yoo, H. S. (2011) Inverse relationship between adipocyte differentiation and ceramide level in 3T3-L1 cells. *Biol. Pharm. Bull.* **34,** 912–916
53. Sprott, K. M., Chumley, M. J., Hanson, J. M., and Dobrowsky, R. T. (2002) Decreased activity and enhanced nuclear export of CCAAT-enhancer-binding protein beta during inhibition of adipogenesis by ceramide. *Biochem. J.* **365,** 181–191
54. Holland, W. L., Brozinick, J. T., Wang, L. P., Hawkins, E. D., Sargent, K. M., Liu, Y., Narra, K., Hoehn, K. L., Knotts, T. A., Siesky, A., Nelson, D. H., Karathanasis, S. K., Fontenot, G. K., Birnbaum, M. J., and Summers, S. A. (2007) Inhibition of ceramide synthesis ameliorates glucocorticoid-, saturated-fat-, and obesity-induced insulin resistance. *Cell. Metab.* **5,** 167–179
55. Choi, J. H., Banks, A. S., Estall, J. L., Kajimura, S., Boström, P., Laznik, D., Ruas, J. L., Chalmers, M. J., Kamenecka, T. M., Blüher, M., Griffin, P. R., and Spiegelman, B. M. (2010) Anti-diabetic drugs inhibit obesity-linked phosphorylation of PPARγ by Cdk5. *Nature* **466,** 451–456